Lactose Binding to the *E. coli* Symport Protein *Lac* Permease

Thesis by
Denise Lynne Worthen

In Partial Fulfillment
of the Requirements for
the Degree of Master of Science

California Institute of Technology
Pasadena, California

1989

(submitted April 28, 1989)

ABSTRACT

Lac permease is a symport protein which responsible for the active accumulation of lactose in *E. coli*. The protein utilizes the energy from the downhill translocation of protons to drive uphill accumulation of lactose. This work reports the direct measurement by proton NMR of lactose binding to *lac* permease of *E. coli* membrane vesicles. The technique allows the determination of the K_d of lactose binding to *lac* permease binding sites. The results presented here show that the assay is specific for *lac* permease binding sites and that the assay can distinguish differences in binding affinity for different site specific mutants of *lac* permease. Determination of the Kd for lactose binding is important in determining which residues are important for lactose binding.

INTRODUCTION

Part I: Function and Structure of *lac* Permease

The bacterium *Escherichia coli* is a natural inhabitant of the lower intestine in mammals. In response to the low levels of ingested lactose in the lower intestine, *E. coli* has evolved a system to actively scavenge lactose. The carrier protein responsible for the active accumulation of lactose against a concentration gradient has been named *lac* permease. In addition to lactose (glucose-4-β-D-galactoside) other naturally occurring β-galactosides such as melibiose are also substrates for *lac* permease. High affinity substrates for *lac* permease include o-nitrophenylgalactoside and the several thiogalactosides such as thiomethylgalactoside (TMG), thiopropylgalactoside (TPG) and thiodigalactoside (TDG) (Figure 1).

The accumulation of lactose by *E. coli* is coupled with the movement of protons, demonstrating that *lac* permease is really a symporter; it couples the transport of β-galactosides and protons (Figure 2). Thus, in the presence of $\Delta\mu_{H^+}$ (interior negative and alkaline) *lac* permease uses the free energy released from downhill H^+ translocation to drive the uphill accumulation of β-galactosides. In the presence of a substrate concentration gradient, the protein uses the free energy from downhill translocation of substrate to drive the generation of $\Delta\mu_{H^+}$. The polarity of the gradient thus generated depends on the direction of the substrate gradient. (1)

The kinetic scheme which describes the catalytic cycle of *lac* permease is shown in Figure 3. The complete cycle corresponds to at least 4 steps: *i)* binding of substrate and H^+; *ii)* translocation of the loaded carrier across the membrane; *iii)* release of substrate and H^+; *iv)* return of the unloaded carrier. Studies on efflux, exchange and counterflow in *E. coli* membrane vesicles (2,3), and in proteoliposomes reconstituted with *lac* permease from *E. coli* (4,5) have provided evidence which is consistent with the following points. 1) The rate determining step for downhill efflux of lactose corresponds to the return of the unloaded carrier. 2) The carrier recycles in the protonated form during exchange and counterflow. 3) Efflux occurs by an ordered mechanism

Figure 1. Substrates for *lac* permease.

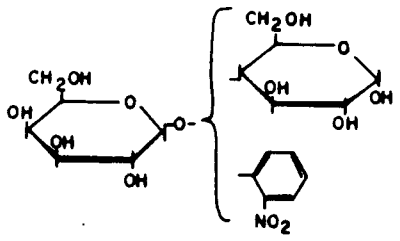

LACTOSE

o-NITROPHENYLGALACTOSIDE

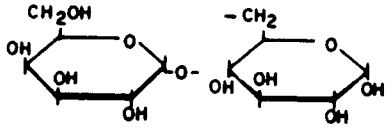

MELIBIOSE

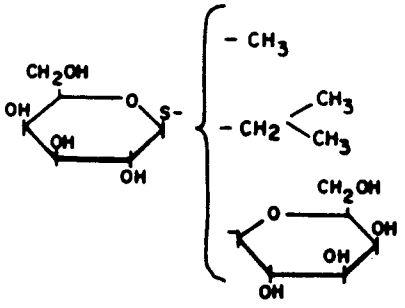

THIOMETHYLGALACTOSIDE

THIOISOPROPYLGALACTOSIDE

THIODIGALACTOSIDE

Figure 2. Lactose transport in *E. coli*. (A) Uphill lactose transport in response to $\Delta\mu_{H^+}$. (B) Uphill H^+ transport in response to inward directed lactose gradient. (C) Uphill H^+ transport in response to outward directed lactose gradient (1).

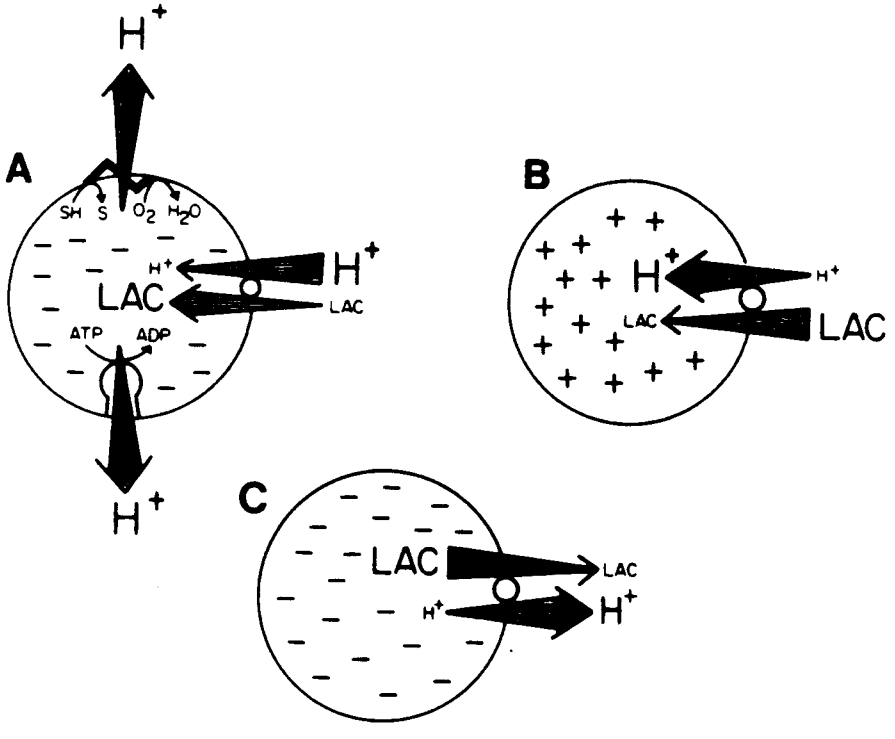
A
H+
SH
S
O2
H2O
H+
LAC
H+
LAC
ATP
ADP
H+
B
H+
H+
LAC
LAC
C
LAC
LAC
H+
H+

Figure 3. Schematic representation of the cyclic reactions catalyzed by *lac* permease (1).

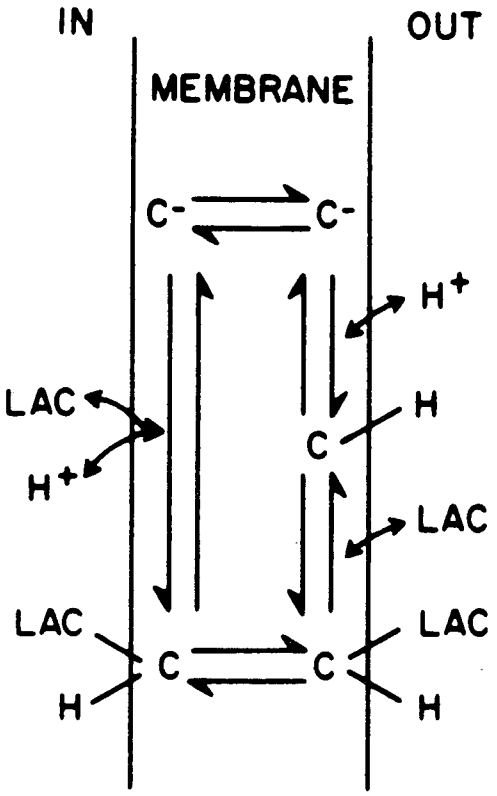
IN
OUT
MEMBRANE
C-
C-
H+
LAC
H
H+
C
LAC
LAC
LAC
C
C
H
H

whereby lactose is released first, followed by release of the H^+. 4) The reactions catalyzed by the unloaded carrier involve the net movement of negative charge.

The membrane protein *lac* permease which accomplishes this symport of lactose and H^+'s is the product of a single gene *lac Y* (6). The gene has been cloned, and the product of the gene purified and reconstituted in a fully active form, proving that the protein *lac* permease is the single protein necessary for β-galactoside accumulation in *E. coli*. (7,8). Buchel *et al* (9) determined the nucleotide sequence of the *lac Y* gene. The primary structure of *lac* permease is predicted to consist of 417 residues yielding a molecular weight of 46,504.

Based on circular dichroism studies and a hydropathy profile of the protein Foster *et al* (10) have proposed a secondary structure model for *lac* permease of at least 12 α-helical segments of approximately 24 amino acid residues each. The model implicitly assumed that these segments span the membrane in a zig-zag fashion (Figure 4). Using Raman spectroscopy and a method for structural prediction which allowed for amphipathic helices, Vogel *et al* (11) have postulated a different model for the folding of *lac* permease in the membrane (Figure 5). Agreeing that *lac* permease has a significant α-helical content (~70%), these authors postulated a model of the protein consisting of 14 regions of α-helical content. Of these 14 segments, 10 were predicted to be hydrophobic or amphipathic and therefore were assigned as membrane spanning α-helices. The remaining four segments were classified as more hydrophilic and therefore were not predicted to be membrane spanning. The 10 hydrophobic or amphipathic helices were postulated to form an outer ring in the membrane with their hydrophobic faces towards the lipids and their more hydrophilic faces towards the core of the ring. The four remaining hydrophilic helices were postulated to fill the interior of the ring and contain the sugar binding site.

Goldkorn, *et al* (12) showed that proteolysis treatment of *E. coli* membrane vesicles containing *lac* permease inactivated the transport capabilities of *lac* permease indicating that the protein must transverse the bilayer. In addition, it was shown by photo-affinity labeling experiments that proteolysis had no effect on the ability of *lac* permease to bind substrate. The conclusion was that the substrate binding site was embedded in the membrane bilayer. Page and

Figure 4. Secondary structure model of *lac* permease. Hydrophobic segments are shown in boxes as transmembrane, α-helical domains connected by hydrophilic segments (3).

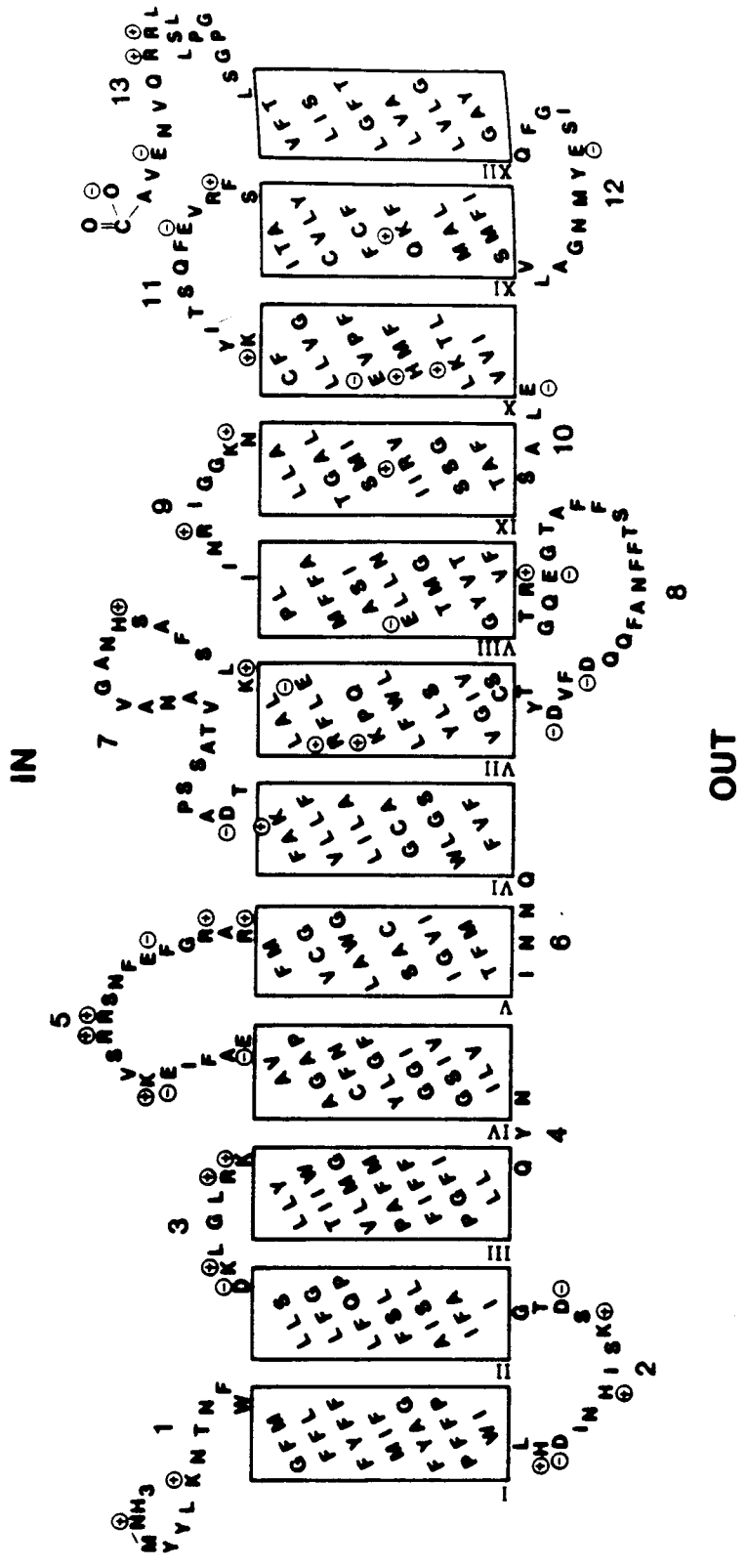
IN
OUT

Figure 5. Model for the folding of *lac* permease in the membrane. Solid rectangles represent predicted membrane spanning α-helices which are oriented so that their most hydrophilic sides, indicated by bold-faced lettered residues, face the observer. Dashed rectangles represent regions which are not predicted to be membrane spanning α-helices. Zig-zags symbolize β-strands and stars symbolize β-turns. Circles and squares indicate positively and negatively charged residues, respectively (11).

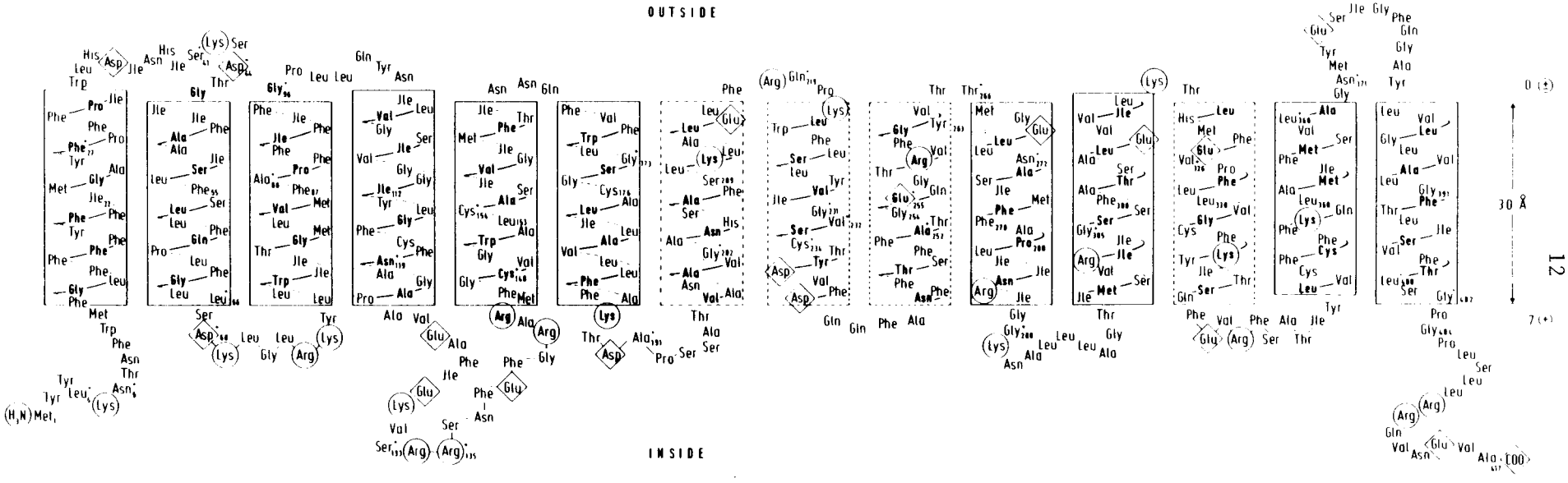
OUTSIDE
INSIDE
30 Å
0 (±)
7 (+)
1
2
3
4
5
6
(7)
(8)
(9)
10
11
(12)
13
14

Rosenbusch (13) have examined the topography of *lac* permease by labeling both the membrane embedded and exposed portions of the protein. These authors concluded that the accessibility of the protein at the membrane surface is greater on the cytoplasmic side and that substrate binding appeared to be accompanied by some residues becoming more exposed and others more buried. The authors concluded that for the first 150 and the last 200 residues the prediction (10) of α-helical, membrane spanning segments appeared valid. However, in the central 1/3 of the protein the packing was more complicated than simple membrane spanning α-helices. Using the accessibility of permease-bound fluorphores to collisional quenchers, Mitaku *et al* (14) provided evidence that the galactoside binding site was embedded in the protein and that the binding site was accessible to the aqueous phase.

Support for a membrane embedded substrate binding site accessible to the aqueous phase is provided by recent experiments on the physical appearance of *lac* permease. Li and Tooth (15) have recently purified active *lac* permease in a ratio of 4-5 mol phospholipid per mol *lac* permease. Below this ratio, the protein was found to form long filamentous structures which associate laterally to form sheets. The filaments were not helical but ribbon-like and appeared to be composed of two subunit structures separated by a cleft. The substrate binding site was postulated to reside in this cleft. A freeze fracture microscopy study of *lac* permease (16) has revealed that the protein appears in the membrane as a oblong shape containing a notch. Using the assumption of 12 α-helical segments (10), this structure led the authors to postulate a model of the helical packing of the protein which assumed a rectangular shape with unsymmetrical packing of α-helices creating a cleft for the substrate binding site (Figure 6).

Part II: Isolation of Residues Critical for Activity of *lac* Permease

Functional studies have allowed the elucidation of the catalytic cycle of *lac* permease and structural studies have provided some insight into the nature of the substrate binding site in the protein. One approach that has been used in an attempt to determine the actual mechanism by which

Figure 6. Schematic drawing of a possible packing arrangement of 12 α-helices in *lac* permease with a cleft for substrate (S) binding.The model is drawn approximately to scale with an α-helix diameter of 1.1 nm and a substrate (lactose) diameter of .70 nm (10).

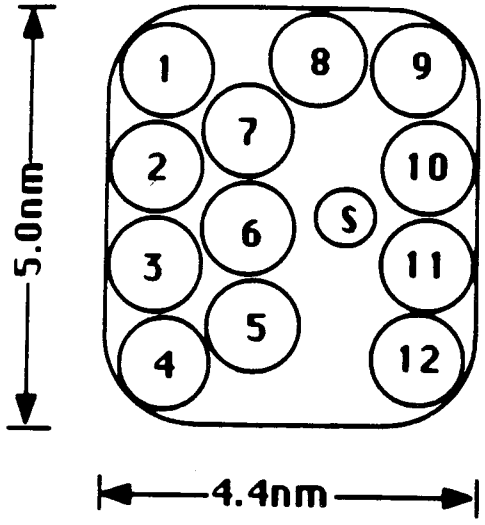
1
8
9
7
2
10
S
6
3
11
5
4
12
5.0nm
4.4nm


H
L
S
1.1nm
0.84nm
0.70nm

lactose and H^+'s are symported by *lac* permease is site-directed mutagenesis. This technique allows the modification of a specific amino acid residue(s) in the protein and can be used to determine the residue(s) in the protein which are in some way critical for transport activity.

The use of site directed mutagenesis has been used extensively by Kaback and collaborators who have assayed the ability of *lac* permease mutants to accomplish facilitated diffusion, efflux, exchange, entrance counterflow and active accumulation of lactose. The ability to catalyze facilitated diffusion (accumulation of lactose down a concentration gradient) was distinguished by the growth of red *E. coli* colonies on lactose-loaded eosin methylene blue (EMB) indicator plates. Efflux and exchange were assayed by following the time-course loss of pre-loaded radioactively labeled lactose in the absence of external lactose (efflux) or in the presence of external equimolar concentrations of unlabeled lactose (exchange) (Figure 7 A and B). Counterflow was assayed by the transient influx of radioactively labeled lactose into vesicles pre-loaded with unlabeled lactose (Figure 7C). Active transport of lactose was assayed by the accumulation of radioactively labeled lactose against a concentration gradient (Figure 7D).

Based on substrate protection against inactivation by n-ethyl maleimide, Fox and Kennedy (6) first postulated that there was an essential cysteine in *lac* permease. Subsequently, the eight cysteine residues were systematically replaced by site directed mutagenesis and the effect of the replacement on transport activity measured. In particular, *E. coli* colonies containing the Cys148 mutation were able to catalyze facilitated diffusion and vesicles exhibited wild-type initial rates and steady-state accumulation levels of lactose (17). Replacement of Cys154 with Gly154 resulted in permease which was completely inactive and Ser154 was severely deficient. However both Cys154 mutants bound the high affinity ligand p-nitrophenylgalactoside normally (18). Menick *et al* (19) present a summary of the role of the eight cysteine residues in *lac* permease based on site-directed mutagenesis studies. Of the eight cysteine residues, only Cys154 was found to be essential for transport activity.

An important role for histidine residues has also been postulated based on inactivation of *lac* permease transport activity after photo-oxidation with rose bengal or treatment with

Figure 7. Experimental schemes for following (A) efflux, (B) exchange, (C) entrance counterflow, and (D) active accumulation of lactose by *lac* permease in *E. coli* membrane vesicles. **L** denotes a lactose molecule and **L*** denotes a radioactively labeled lactose molecule.

A

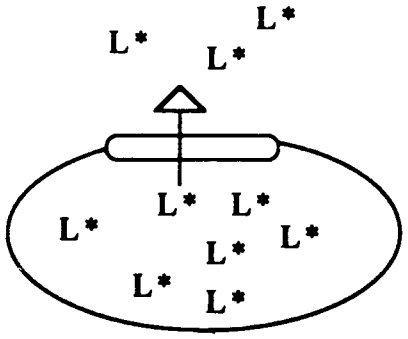

B

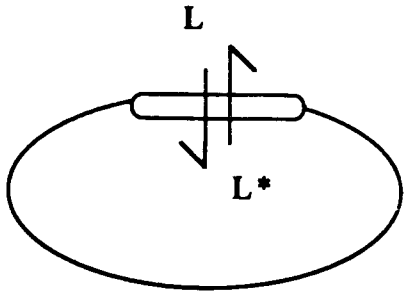

C

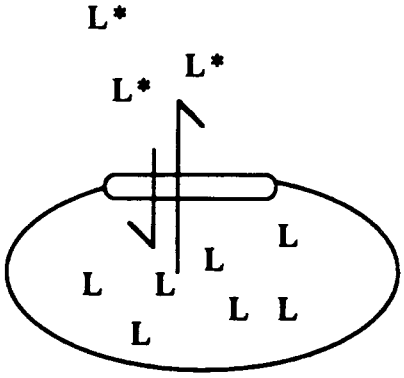

D

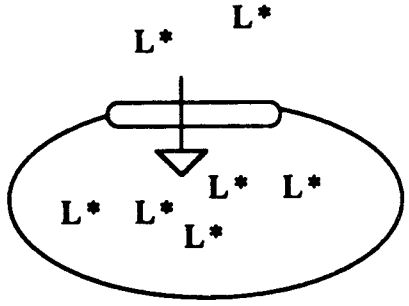

diethylpyrocarbonate (20-22). The effect has been shown to be the result of modification of two of the four histidine residues in *lac* permease (22). All four histidine residues have been replaced using site-directed mutagenesis (23,24) and the results are summarized below. Replacement of histidine residues 35 or 39 by arginine resulted in *E. coli* colonies which were able to catalyze facilitated diffusion. No effect on either the initial rate or steady state accumulation levels of lactose was found in either Arg35 or Arg39. Replacement of His205 and His322 had differing effects. Colonies containing the mutation Arg205 were unable to catalyze facilitated diffusion and showed negligible initial rates of lactose uptake and negligible steady state accumulation levels. Colonies containing the mutation Arg322 were able to catalyze facilitated diffusion at high (25 mM) lactose concentrations but not at lower lactose concentrations (12.5 mM or 6.5 mM). However, like Arg205, Arg322 was unable to accumulate lactose. In addition, permease containing Arg322 was purified and reconstituted into proteoliposomes and was shown to catalyze facilitated diffusion at high lactose concentrations. However, the diffusion of lactose into the proteoliposomes was not accompanied by alkalinization of the medium; the movements of lactose and protons were uncoupled in the Arg322 mutant. Furthermore, replacement of His322 with either Asn322 or Gln322 yielded a permease with the same characteristics as Arg322. However, replacement of His205 with either Asn205 or Gln205 yielded colonies which were able to catalyze facilitated diffusion and which were able to catalyze accumulation of lactose. Thus, at the 322 position it appears that histidine is essential for activity while at the 205 position there is no such rigorous condition.

In the model proposed by Foster *et al* (10) of the secondary structure of *lac* permease in the membrane His322 and Glu325 reside in putative helix X. It was postulated that His322 and Glu325 could be in close enough proximity to hydrogen bond and that together His322 and Glu325 could function as a charge relay system. This mechanism has been used to describe chymotrypsin function (25). Accordingly, Glu325 was replaced with Ala325 (26). It was found that *lac* permease with Ala325 was unable to catalyze efflux or uphill lactose accumulation and yet was able to catalyze exchange and counterflow. Combined with the results from the His322

mutant, it was proposed that mutation of His322 resulted in permease which was unable to catalyze steps in the kinetic cycle involving protonation or deprotonation and that mutation of Glu325 resulted in permease which was unable to catalyze net H^+ translocation.

In an attempt to expand on the charge relay mechanism hypothesis, it was shown by molecular modeling that Arg302 could be in a position to function in concert with His322 and Glu325 as a charge relay triad (Figure 8). Thus, Arg302 was replaced with Leu302 (27). Permease with Leu302 was able to catalyze facilitated diffusion at high lactose concentrations but was unable to catalyze active transport, efflux, exchange or counterflow. Thus, the mutations Leu302 and Arg322 cause the same loss of function *lac* permease.

Part III: Isolation of Residues Critical for Binding of Lactose to *lac* Permease

While the kinetic studies outlined above (Table 1) are useful in studying the effects of various site specific mutations, it is difficult to resolve from such studies whether the effect of a particular mutation directly involves the ability of *lac* permease to bind lactose or whether the mutation effects a step in the catalytic cycle removed from lactose binding. In an attempt to further examine the effect of the various site-directed mutations in *lac* permease on the transport mechanism, the binding of lactose to *lac* permease has been directly measured. Thus, the effect of the site specific mutations on the binding of lactose can be isolated. The technique used exploits the relationship between the nuclear Overhauser effect (NOE) between two protons and the environment of the two protons. The technique has been used to detect the binding of a sugar substrate to its transporter (28) and a brief explanation of the technique is outlined here.

The intramolecular nuclear Overhauser effect arises when any two protons on the same molecule lie close enough so that their magnetic dipoles interact. Under these circumstances, irradiation at the NMR frequency of one of these protons will effect the intensity of the NMR resonance of the other proton by a factor $1 + f_I(S)$ where $f_I(S)$ is given by (28)

Figure 8. Secondary structure model of putative helices IX and X of *lac* permease modified to bring Arg302 into proximity with His322 and Glu325 (25).

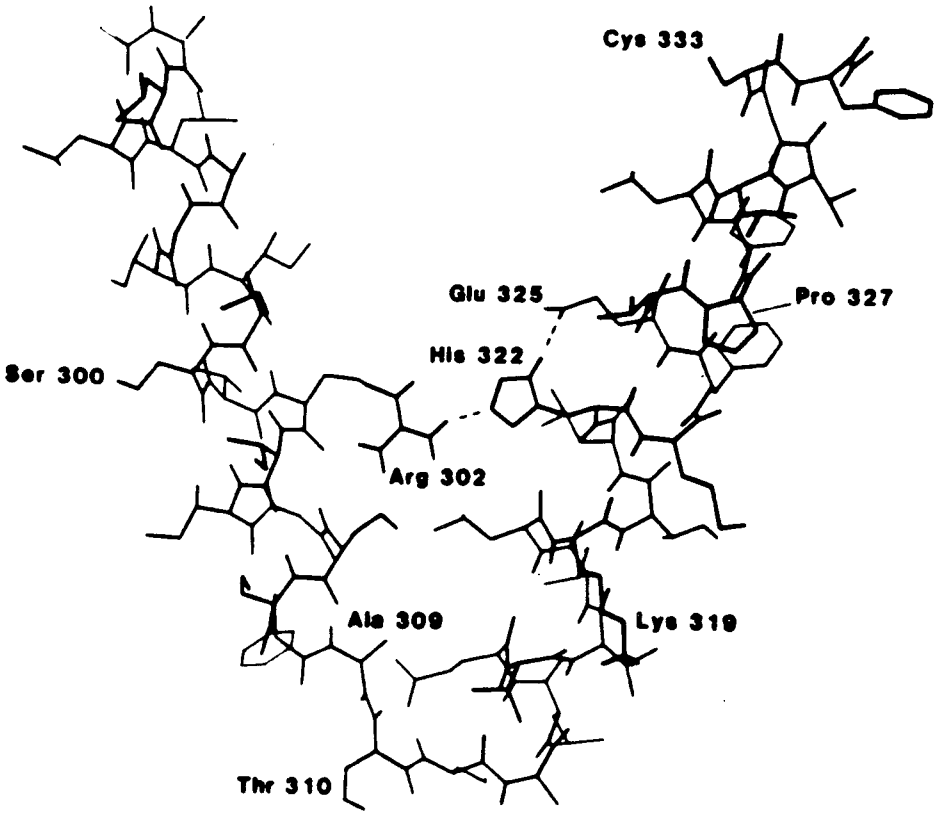
Cys 333
Glu 325
Pro 327
His 322
Ser 300
Arg 302
Ala 309
Lys 319
Thr 310

Table 1. Summary of effects of site directed mutagenesis on activities of *lac* permease[1]

Mutation[2]	Facilitated Diffusion	Efflux	Exchange	Counterflow	Active Transport
lac Y $^-$	-	-	-	-	-
wild-type	+	+	+	+	+
Cys148⇒Ser148	+				+
Cys154⇒Gly154	-				-
His35⇒Arg35	+				+
His39⇒Arg39	+				+
His205⇒Arg205	-				-
His205⇒Gln205	+				+
His205⇒Asn205	+				+
His322⇒Arg322	+[3,4]				-
His322⇒Gln322	+[3]				-
His322⇒Asn322	+[3]				-
Arg302⇒Leu302	+[3,4]	-	-	-	-
single histidine (His322)	+	+	+	+	+
single histidine (His322) Glu325⇒Ala325	+[3]	-	+	+[5]	-

1) Blanks indicate that no experimental results are available
2) Results are for RSO vesicles only
3) Facilitated diffusion occurs at lactose concentrations ≥ 25 mM
4) Facilitated diffusion of lactose is uncoupled from H^+ translocation
5) Counterflow ability is essentially identical to wild-type except that internal concentration of labeled lactose is maintained for prolonged periods

$$f_I(S) = \left(\frac{\gamma_S}{\gamma_I}\right)\left(\frac{\overline{(W_2 - W_0)}}{\overline{(W_2 + W_{1I} + W_2)}}\right) \qquad [1]$$

where I and S are the observation and irradiation nuclei, respectively; W_2, W_{1I} and W_0 are the double, single and zero quantum transitions probabilities for the I, S spin pair; and the numerator and denominator are separately averaged over the environments sampled rapidly on the NMR timescale. For a rapidly tumbling molecule in solution, Eq. [1] reduces to $\gamma_S/2\gamma_I = 0.5$. For a molecule in a slowly tumbling macromolecular binding site, Eq. [1] reduces to $-\gamma_S/\gamma_I = -1.0$ Therefore, if a molecule in solution rapidly samples a macromolecular binding site(s) such that the exchange between the free solution state and the bound state is rapid on the NMR timescale, the observed NOE will be a weighted average of the free solution NOE and the bound state NOE. If the concentration of bound ligand is much smaller than the total ligand concentration and if there is only one type of binding site, the relationship between the %NOE observed and the K_d of the binding site has been shown (29) to be

$$\frac{(\eta - \eta_f)}{P} = R\left(\frac{1}{K_d}\right)\left(\frac{1/L}{1/L + 1/K_d}\right) \qquad [2]$$

where η is %NOE of the observed peak in presence of protein, η_f is the %NOE of the peak in the absence of protein, P is the total protein concentration and L is the total lactose concentration. The multiplicative factor R is given by

$$\left(\frac{\rho}{\rho_f}\right)\eta' Z$$

where ρ is the relaxation rate of lactose in the binding site, ρ_f is the relaxation rate of lactose in the free state, η' is the NOE of lactose in the binding site, and Z is defined by

$$E = ZP$$

where E is the concentration of binding sites and P is the total protein concentration.

MATERIALS AND METHODS

Preparation of membrane vesicles - Membrane vesicles containing *lac* permease were generously provided by Dr. H.R. Kaback and co-workers. The membrane samples are referred to in the following shorthand notation. T184 membranes were essentially devoid of *lac* permease. T206 membranes contained wild-type permease. The remainder of the membranes were denoted by the position of the mutation and the one letter amino acid code for the mutation made. Thus, mutation of residue 322 to arginine was denoted as R322. Samples containing a single remaining histidine at the 322 postition were denoted as RQHE if adjacent residue 325 were glutamic acid and RQHA if residue 325 had been replaced by alanine.

Samples of right-side-out (RSO) vesicles were provided 100 mM KPi, pH 6.6 buffer. Samples of inside-out (ISO) membrane vesicles were provided in 50 mM KPi, 1 mM DTT, 3 mM $MgSO_4$, 1.5 mM PMSF, pH 7.5 buffer. Exchangeable protons were depleted by the following procedure. On the day of the NMR experiment, aliquots of approximately 15-20 mg of protein were thawed. The thawed samples, either RSO or ISO, were diluted 1:30 with 100 mM KPi, 10 mM $MgSO_4$, pH 7.5 buffer and allowed to stir at room temperature for 30 min. The remainder of the preparation was carried out at 0-4 ^{o}C. RSO membranes were pelleted by centrifugation at 16,000 rpm for 20 min in a Sorvall SS-34 rotor. The pellet was resuspended in 1-2 ml of 100 mM KPi, 10 mM $MgSO_4$, pH 7.5 buffer prepared in 99.9% D_2O (D_2O buffer) and repelleted at 13,000 rpm for 8 min in an HBI Micro Centrifuge. This D_2O buffer wash was repeated three times. After the final wash, the pellet was resuspended to approximately 700 µl total volume in D_2O buffer. ISO membrane vesicle samples were pelleted at 40,000 rpm for 90 min in a Ti60 rotor after the room temperature buffer equilibration. The pellet was resuspended in D_2O buffer (1-2 ml) and repelleted in an SW50.1 rotor at 40,000 rpm for 90 min. This D_2O buffer wash was repeated twice. After the second spin, the pellet was resuspended to 700 µl in D_2O buffer.

NMR sample preparation- In all experiments, samples were made of varying lactose concentration and identical protein concentration. Samples were made by the following procedure. A 375 mM lactose stock solution in D_2O buffer and a 1:10 dilution of this solution were freshly made for each experiment. Each NMR sample contained an appropriate amount of stock or 1:10 lactose solution, 100 µl of membrane preparation, and D_2O buffer to a total volume of 400 µl. Typical final protein concentrations were 3-4 mg/ml. The lactose concentrations were 300 mM, 75 mM, 50 mM, 13 mM, 11 mM and 2.3 mM. After the NMR experiment was performed on these six samples, six additional samples containing intermediate concentrations of lactose were made by mixing these concentrations in the appropriate ratio. For example, the 300 mM sample and the 75 mM sample were mixed to yield concentrations of 230 mM and 150 mM. The additional concentrations made by mixing were 230 mM, 150 mM, 37 mM, 25 mM, 7.8 mM and 5.0 mM. The samples were stored on ice at all times.

NOE Difference Spectroscopy - The NMR spectra were obtained using a Bruker 500 MHz spectrometer. The samples were run at ambient temperature with sample spinning. The NOE difference spectra were generated by a modification of the Bruker automation library program NOEDIFF.AUR. The program was modified in order to accommodate a Redfield pulse sequence for suppression of the residual water peak. The Redfield pulse was a composite pulse of the form (P2 PH1 P1 PH2 P4 PH1 P1 PH2 P3 PH1) where P1, P2, P3. and P4 were the pulse lengths and PH1, PH2, PH3, and PH4 were the pulse phases. The placement of the Redfield pulse was optimized for each spectrum by adjustment of the offset parameter O1. Adjustment of the excitation pulse lengths P1, P2, P3 and P4 was not usually necessary. The standard Redfield pulse was O1~ 8100 Hz, P1=100 µs, P2=200 µs, P3=200 µs, P4= 400 µs.

The modified NOEDIFF.AUR program generated both on and off resonance spectra by variation of the irradiation frequency O2. Long term averaging of the spectra was accomplished by cycling through the irradiation frequency list.The standard acquisition parameters for the NOE difference spectra were a time domain of 16K and a spectral width of 4807 Hz. This gave an acquisition time of 1.7 sec. For proper functioning of the automation program, the pulse

width and relaxation delay were set at 0.0 sec. The position of the peak to be irradiated varied slightly (± 5 Hz) between experiments. Therefore, the on resonance irradiation frequency was optimized for each expeiment depending on the exact position of the (largest) peak near O2~ 8450 Hz. The off resonance irradiation frequency was set at O2~ 6933 Hz. The irradiation power level was 35L, the irradiation time was 3.0 sec, and the relaxation time between scans was .1 sec. The number of cycles made through the irradiation frequency list was set at a minimum of 3 and a maximum of 16. Four dummy scans were made at the start of each cycle in order to allow the build-up of the NOE to steady-state levels. The number of scans was set at either 8 scans for lactose concentrations of 75 mM and higher and 16 scans for the remaining concentrations so that the minimum number of scans was 24 (3 x 8) and the maximum number was 256 (16 x 16). The FIDs were zero filled to 32K and the same absolute intensity scaling of the FIDs for each on/off resonance pair was set. Each on/off resonance pair was Fourier transformed and phased and the NOE difference spectrum was generated by subtracting the on resonance spectrum from the off resonance spectrum. Both the off resonance peak and the difference peak were plotted.

NMR sample analysis - After the NMR spectra were obtained, the protein concentration of the samples was determined by the modified Lowry procedure (31).

NMR spectrum analysis - The %NOE was determined by dividing the the NOE difference peak area by the off resonance peak area. The areas were measured using a planimeter (Keuffel & Esser Co. model 620005). The areas of both the off resonance peak and the difference peak were measured three times, and the average was used as the value of the peak area.

RESULTS

500 MHz Spectrum of Lactose- The ^1H spectrum of pure lactose in KPi/D_20 buffer is shown (Figure 9). The spectrum has been referenced to TSP (0.0 ppm) in the same buffer. A Redfield pulse was applied to reduce the intensity of the HOD peak at ~4.80 ppm. The spectrum has been partially assigned (30).

Evidence of NOE in the Spectrum of Lactose - In the absence of protein, irradiation at O2~ 8450 Hz results in the increase in intensity of the $H_{2\beta}$Glu peak of lactose (Figure 10A). The %NOE increase in intensity of this peak (ηf) was measured to be 8.5 ± 1.6. This value was found to hold for lactose concentrations between 300 mM and 13 mM.

Evidence of lactose binding in presence of lac permease - The %NOE for the $H_{2\beta}$Glu peak of lactose in the presence of membranes containing *lac* permease (η) is less positive than the mean value of 8.5% which occurs for free lactose in solution (Figure 10B). Evidence that this is due to the rapid exchange of lactose between a binding site on the *lac* permease molecule and the solution is provided by the lack of any such effect when T184 membranes are used (see below). The %NOE of the $H_{2\beta}$Glu peak of lactose in the presence of membranes containing *lac* permease is a function of lactose concentration (Appendix I).

Determination of K_d from NOE data - The lactose concentration dependence of the NOE effect in the presence of *lac* permease was used to generate a value of the disassociation constant for the lactose molecule in the binding site. The data was fit to Eqn. [2] using a non-linear least squares fitting routine of the appropriate form. The computer fit generated values of $1/K_d$ and R.The values of K_d are given in Table 2. On average, 3-5 data sets were compiled for each mutant. Unless otherwise noted, each data set was fit to Eq. [2] individually. Table 2 gives the average K_d and the standard deviation of the K_d for the computer fits to the individual data sets. In the cases of S148, R205 and R322 the individual fits gave widely varying values of K_d; the K_d 's are therefore reported as ranges. In two cases where the binding was weak but measureable

Figure 9. Lactose 500 MHz ^{1}H spectrum. Lactose concentration 50 mM; 25 ^{o}C.

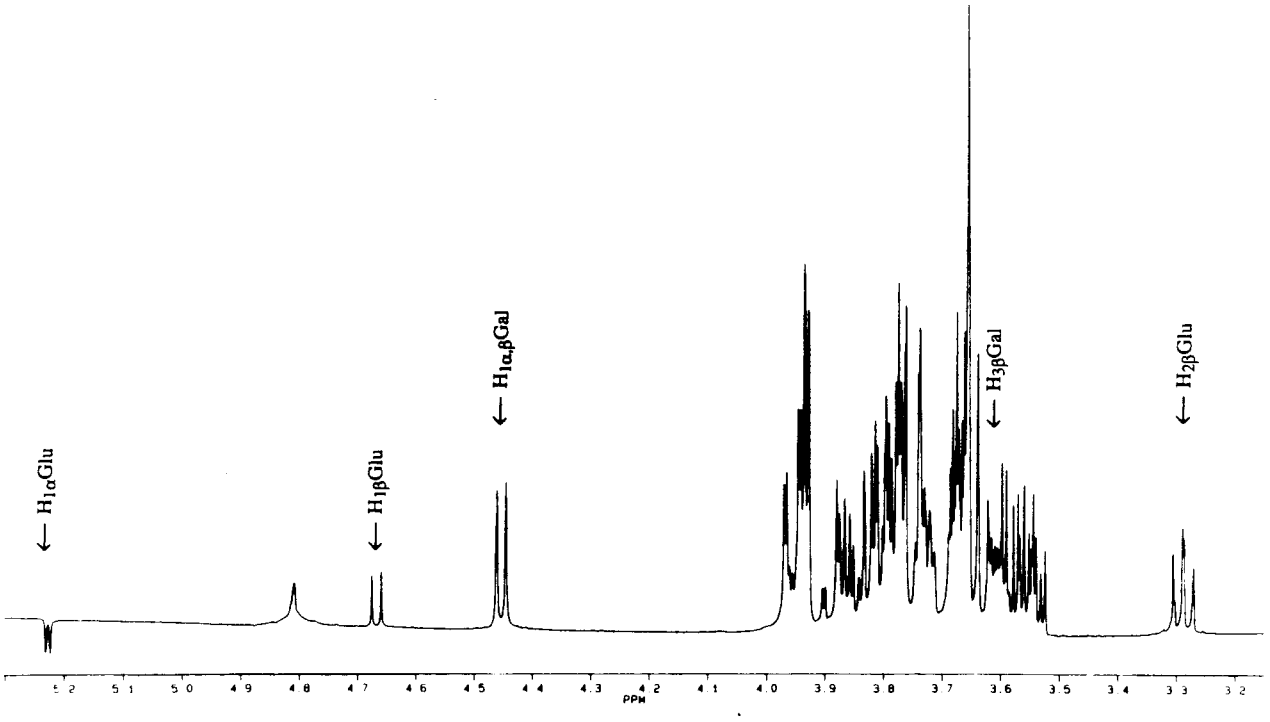
← H1αGlu
← H1βGlu
← H1α,βGal
← H3βGal
← H2βGlu
5.2 5.1 5.0 4.9 4.8 4.7 4.6 4.5 4.4 4.3 4.2 4.1 4.0 3.9 3.8 3.7 3.6 3.5 3.4 3.3 3.2
PPM

Figure 10. The effect of lactose binding sites on the lactose ^{1}H NOE difference spectrum. Shown is the off resonance and NOE difference spectra of a) lactose and b) lactose in the presence T206 membranes. For both (A) and (B), the difference spectrum is scaled relative to the off resonance spectrum by a factor of four. Lactose concentration 13 mM (A,B) and protein concentration 3.3 mg/ml (B); 25 ^{o}C

A

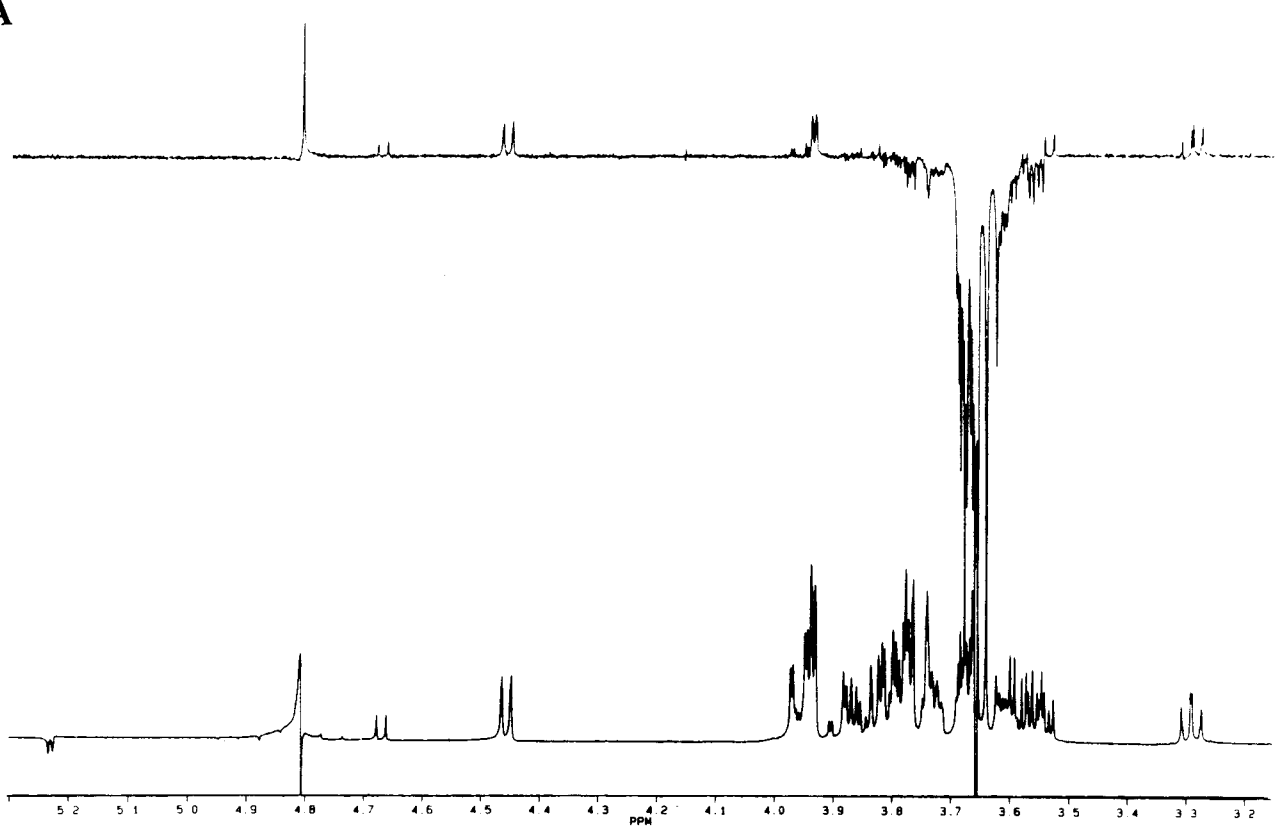
5.2 5.1 5.0 4.9 4.8 4.7 4.6 4.5 4.4 4.3 4.2 4.1 4.0 3.9 3.8 3.7 3.6 3.5 3.4 3.3 3.2
PPM

B

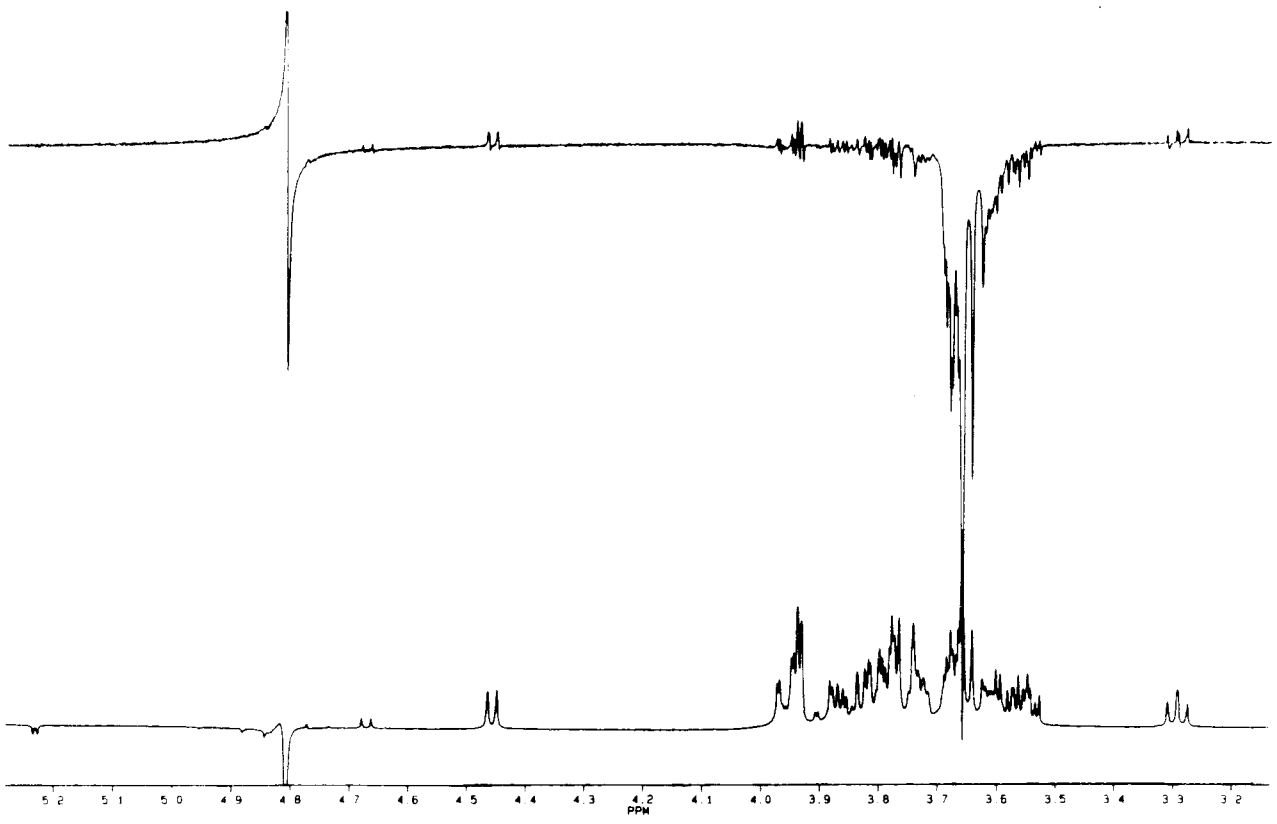
5.2 5.1 5.0 4.9 4.8 4.7 4.6 4.5 4.4 4.3 4.2 4.1 4.0 3.9 3.8 3.7 3.6 3.5 3.4 3.3 3.2
PPM

(T206,ISO and L302,RSO), it was difficult to fit each individual data set to Eq. [2] due to the weak dependence of the NOE on lactose concentration. In these two cases the data sets were combined and the combined data was fit to Eq. [2]. Therefore no standard deviation of the K_d's for T206,ISO and L302,RSO are reported. In the case of T184, RSO and T184, ISO, the data could not be fit to Eq. [2]. It appeared that the binding of lactose to T184 membrane vesicles was so weak that the there was no functional dependence of %NOE on the concentration of lactose. The values of K_d for T184, RSO and T184, ISO are therefore reported as $\geq$ 25000 mM; that is, it was assumed that the upper limit on the ability of the computer program to fit the data to Eq. [2] was represented by the fit to the data for T206,ISO. The data for all the membrane samples tested and the computer fits to the data are presented in Appendix I.

Goodness of Fit - The goodness of fit was found for each computer fit to Eq. [2] by the following formula

$$GOF = \frac{\left(\frac{\sum(y_{obs} - y_{calc})^2}{N}\right)^{1/2}}{\left|y_{obs(max)} - y_{obs(min)}\right|}$$

where N was the number of data points in the fit.

Table 2: Determination of lactose binding to *lac* permease as determined by NOE difference spectroscopy

Name	Mutation	K_d(mM)
T184,RSO	lac Y^-	≥ 25000
T184,ISO		≥ 25000
T206,RSO	wild-type	34 ± 15
T206,ISO		25000
RQHE,RSO	single histidine mutant (His322)	27 ± 17
RQHA,RSO	single histidine mutant (His322) Glu325 ⇒ Ala325	92 ± 26
S148,RSO	Cys148 ⇒ Ser148	$630 \leq K_d \leq 4200$
R205,RSO	His205 ⇒ Arg205	$29 \leq K_d \leq 110$
R322,RSO	His322 ⇒ Arg322	$200 \leq K_d \leq 630$
L302,RSO	Arg302 ⇒ Leu302	830

DISCUSSION

This study reports the measurement of the K_d of lactose bound to *lac* permease. The method used relies on the magnitude of the NOE between two protons on the lactose molecule when the lactose molecule is in exchange between a free solution state and a binding site on *lac* permease. Thus, the NOE reflects the binding of lactose to binding sites of *lac* permease which are exposed to bulk solution. The use of both right-side-out and inside-out membrane vesicles thus allows the assay of binding to either the outward facing or inward facing binding sites. Importantly, this effect is not due to non-specific binding of lactose to *E. coli* membrane vesicles since the effect is totally absent in membranes which are devoid of permease. This is reflected in the (estimated) value of K_d for both RSO and ISO T184 membranes ($K_d \geq 25000$ mM). Therefore, measurement of the K_d for lactose in the presence of *E. coli* membrane vesicles containing *lac* permease reflects binding of lactose to *lac* permease specifically.

The K_d for lactose binding to wild-type *lac* permease in right-side-out membrane vesicles was found to be 34 ± 15 mM. However, lactose was found to have essentially no affinity for wild-type permease in inside-out vesicles ($K_d = 25000$ mM). In addition, *lac* permease with only a single histidine (RQHE), which is fully active, was found to have essentially identical binding affinity as wild-type permease ($K_d = 27 \pm 17$ mM).

Since the assay used in this study determines the binding of lactose to *lac* permease, the effect of site specific mutations of *lac* permease on the ability of the symporter to bind lactose can be measured. As presented in the introduction, site directed mutagenesis of *lac* permease has already been used in an attempt to determine the importance of specific residues for activity. Such studies, however, are ambiguous for the fact that they do not always distinguish between mutations which affect the ability of *lac* permease to bind lactose and mutations which affect *lac* permease at some other critical step in the transport cycle. A mutation which affects

the ability of the permease to bind lactose will not necessarily be reflected in an assay of permease function for the following reason. If the on/off rate of lactose is much faster than the rate of any other step in the catalytic cycle, then a site specific mutation which affects the binding ability of *lac* permease will appear as an effect on activity only if the mutation results in the on/off rate of lactose becoming comparable to other rates in the catalytic cycle. Conversely, if a site specific mutation has an effect on activity , it does not imply that the effect is related to the ability of the mutant permease to bind lactose.

In this context, the effects of site specific mutations on both binding and activity can be compared. Mutation of Cys148 to Ser148 has no effect on activity. However, the mutation of Cys148 to Ser148 results in a sharp increase in the K_d of lactose over wild-type permease (630 mM $\leq K_d \leq$ 4200 mM). Therefore, Cys148 seems important only for binding of lactose and not for activity of *lac* permease. Mutation of His205 to Arg205 probably has little effect on binding (29 mM $\leq K_d \leq$ 110 mM). However, permease with Arg205 is unable to catalyze lactose accumulation. His205 is critical only for activity. Mutation of His 322 to Arg322 has a strong effect on binding (200 mM $\leq K_d \leq$ 630 mM) and a strong effect on activity. While permease with Arg322 is capable of facilitated diffusion at high lactose concentrations, it is unable to actively accumulate lactose. His322 is critical for both binding of lactose and activity of *lac* permease. Mutation of Arg302 to Leu302 also has a strong effect on binding (K_d = 830 mM) and a strong effect on activity. Permease with Leu302 is unable to catalyze efflux, exchange, counterflow or accumulation of lactose, but like Arg322 can accomplish facilitated diffusion at high concentrations of lactose. Leu302 thus seems critical for both binding and activity. Mutation of Glu325 to Ala325 has little effect on binding ($K_d = 92 \pm 26$ mM) but does affect activity. This mutant is capable of catalyzing exchange, counterflow, and facilitated diffusion at high lactose concentrations. It is incapable of catalyzing efflux or active accumulation of lactose. Therefore, while permease with Ala325 can bind lactose, it is not fully functional.

REFERENCES

1) Kaback, H. R. (1987) *Biochem.* 26 (8), 2710-2706

2) Kaczorowski, G. J. and Kaback, H. R. (1979) *Biochem.* 18, 3691-3697

3) Kaczorowski, G. J., Robertson, D. E., and Kaback, H. R. (1979) *Biochem.* 18, 3697-3704

4) Viitanen, P., Garcia, M. L., Foster, D. L., Kaczorowski, G. J., and Kaback, H. R. (1983) *Biochem.* 22, 25331-2536

5) Garcia, M. L., Viitanen, P., Foster, D. L., and Kaback, H. R. (1983) *Biochem.* 22, 2531-2536

6) Fox, C. F. and Kennedy, E. P. (1965) *Proc. Natl. Acad. Sci. USA* 54, 891-899

7) Newman, M. J., Foster, D. L.,Wilson, T. H., and Kaback, H. R. (1981) *J. Bio. Chem.* 256 (22), 11804-11808

8) Foster, D. L., Garcia, M. L., Newman, M. J., Patel, L., and Kaback, H. R. (1982) *Biochem.* 21, 5634-5638

9) Buchel, D., Gronenborn, B., and Muller-Hill, B. (1980) *Nature* 283, 541-545

10) Foster, D. L., Boublik, M. and Kaback, H. R. (1983) *J. Bio. Chem.* 258 (1), 31-34

11) Vogel, H., Wright, J. K., and Jahnig, F. (1985) *EMBO J.* 4 (13A), 3625-3631

12) Goldkorn, T., Rimon, G., and Kaback, H.R. (1983) *Proc. Natl. Acad. Sci. USA* 808, 3322-3326

13) Page, M. G. P. and Rosenbusch, J. P. (1988) *J. Bio. Chem.* 263 (31), 15906-15914

14) Mitaku, S., Wright, J. K., Best, L., and Jahnig, F. (1984) *Bioch. Biophy. Acta* 776, 247-258

15) Li, J. and Tooth, P. (1987) *Biochem.* 26, 4816-4823

16) Costello, M. J., Escaig, J., Matsushita, K., Viitanen, P.V., Menick, D. R., and Kaback, H. R. (1987) *J. Bio. Chem.* 262 (35), 17072-17082

17) Sakar, H. K., Mennick, D. R., Viitanen, P. V., Mohindar, M. S., and H. R. Kaback (1986) *J. Bio. Chem.* 261 (19), 8914-8918

18) Menick, D.R., Sarkar, H. K., Poonian, M. S., and Kaback, H. R. (1985) *Biochem.* Biophy. Res. Comm. 132 (1), 162-170

19) Mennick, D. R., Lee, J. A., Brooker, R. J., Wilson, T. H., and Kaback, H. R. (1987) *Biochem.* 26, 1132-1136

20) Padan, E., Patel, L., and Kaback, H. R. (1979) *Proc. Natl. Acad. Sci. USA* 76, 6221-6225

21) Garcia, M. L., Patel, L., and Kaback, H.R. (1982) *Biochem.* 21, 5800-5805

22) Patel, L., Garcia, M. L., and Kaback, H.R. (1982) *Biochem.* 21, 5805-5810

23) Puttner, I. B., Sarkar, H. K., Poonian, M. S., and Kaback, H. R. (1986) *Biochem.* 25, 4483-4485

24) Padan, E., Sarkar, H. K., Viitanen, P. V., Poonian, M. S., and Kaback, H. R. (1985) *Proc. Natl. Acad. Sci.USA* 82, 6765-6768

25) Blow, D. M., Birktoft, J.J., and Hartley, B. S. (1969) *Nature* 221, 337-340

26) Carrasco, N., Antes, L. M., Poonian, M. S., and Kaback, H. R. (1986) *Biochem.* 25,4486-4488

27) Mennick, D. R., Carrasco, N., Antes, L. M., Patel, L., and Kaback, H. R. (1987) *Biochem.* 26, 6638-6644

28) Wang, J. F., Falke, J. J., and Chan, S. I. (1986) *Proc. Natl. Acad. Sci. USA* 83, 3277-3281

29) Ross, S. A. (1987) Candidacy report, California Institute of Technology

30) Kamerling, J. P., Dorland, L., van Halbeek, H., and Vliegent-Hart, J. F. G. (1982) *Carbo. Res.* 100, 331-340

31) Lowry, O. H., Rosebrough, N. J., Farr, A. L., and Randall, R. J. (1951) *J. Bio. Chem.* 193, 265-275

APPENDIX I

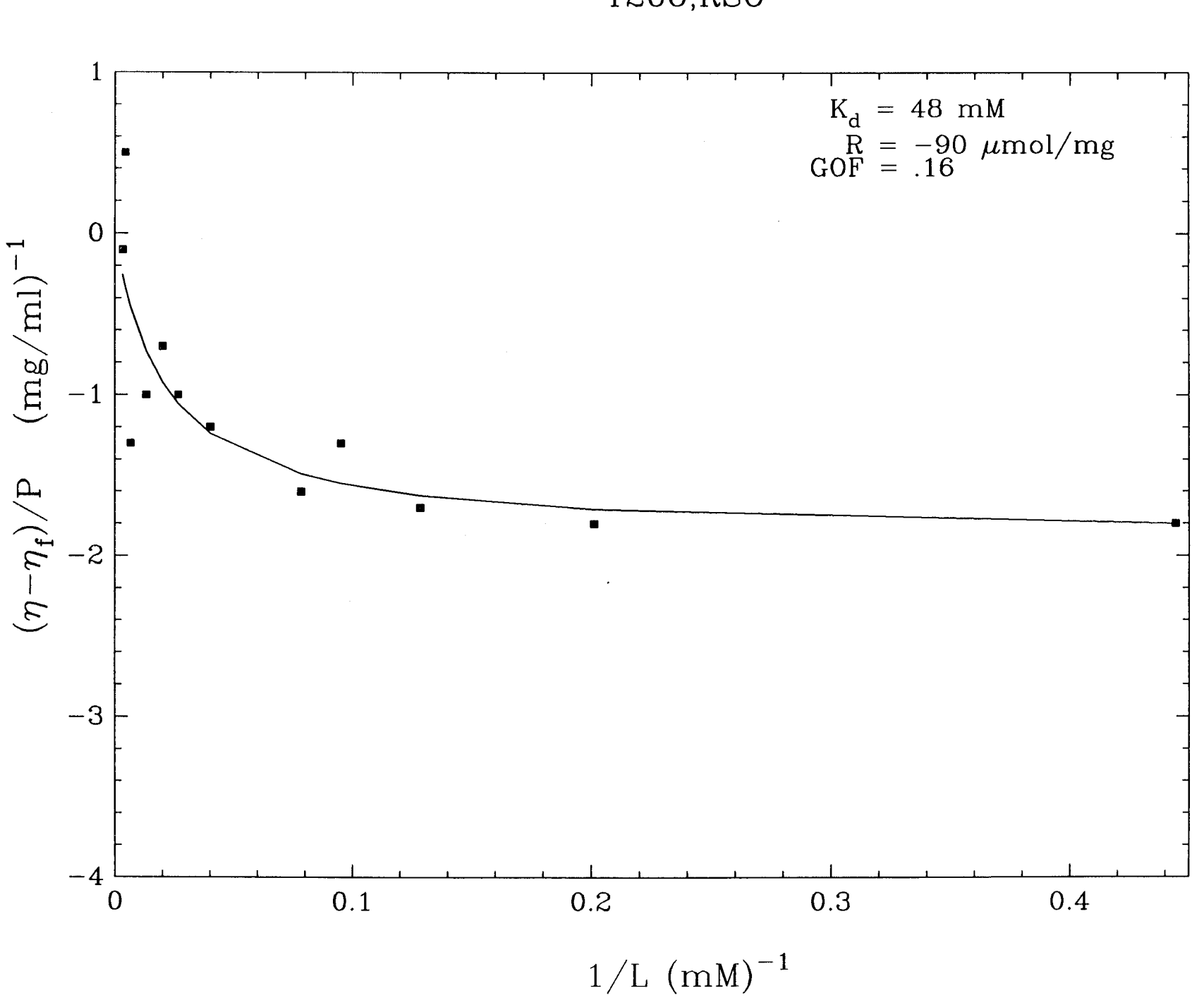
T206,RSO
K_d = 48 mM
R = −90 μmol/mg
GOF = .16
$(\eta-\eta_f)/P$ $(mg/ml)^{-1}$
1
0
−1
−2
−3
−4
0
0.1
0.2
0.3
0.4
$1/L\ (mM)^{-1}$

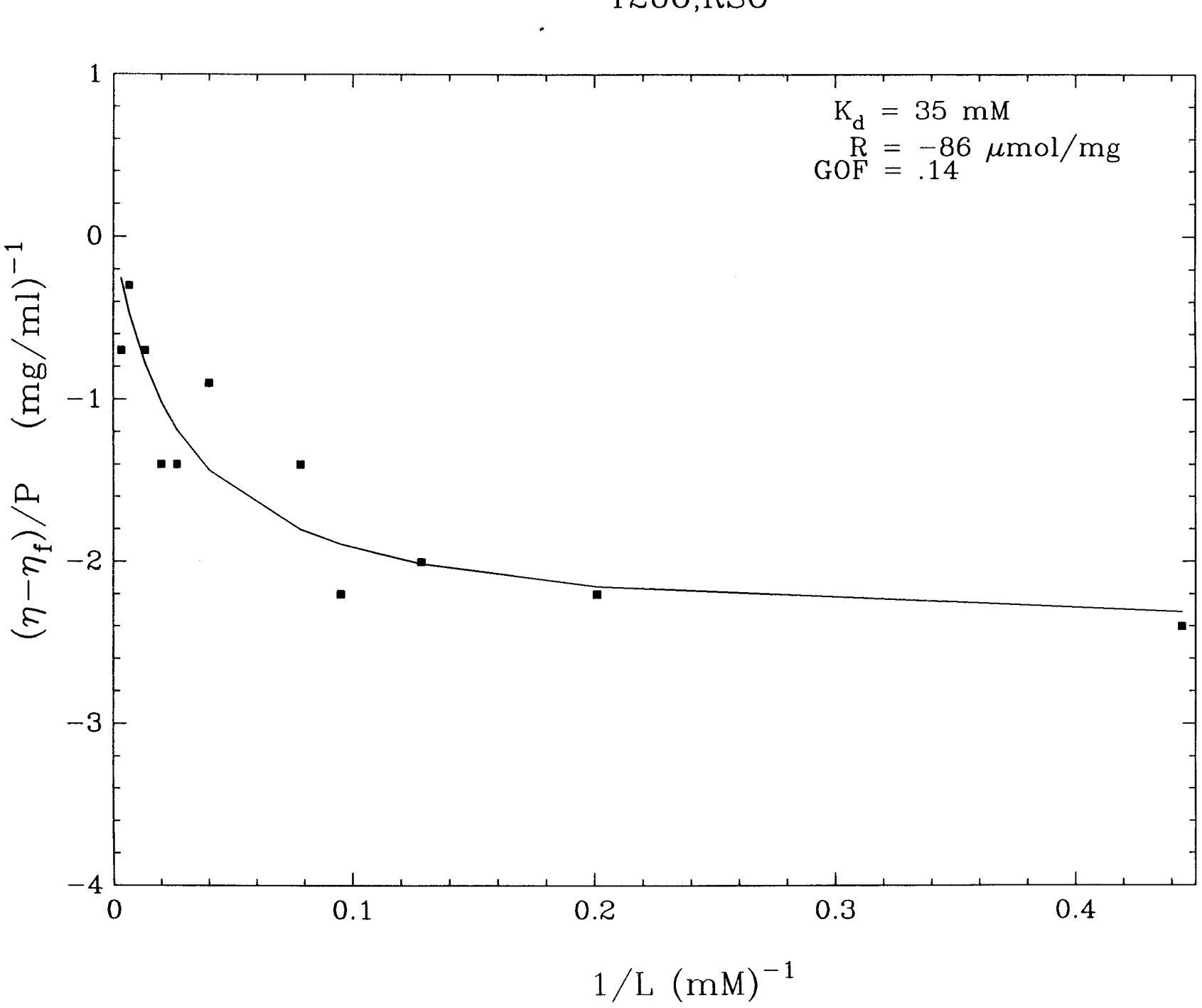
T206,RSO
K_d = 35 mM
R = −86 μmol/mg
GOF = .14
$(\eta-\eta_f)/P$ (mg/ml)$^{-1}$
1/L (mM)$^{-1}$
1
0
−1
−2
−3
−4
0
0.1
0.2
0.3
0.4

T206,RSO

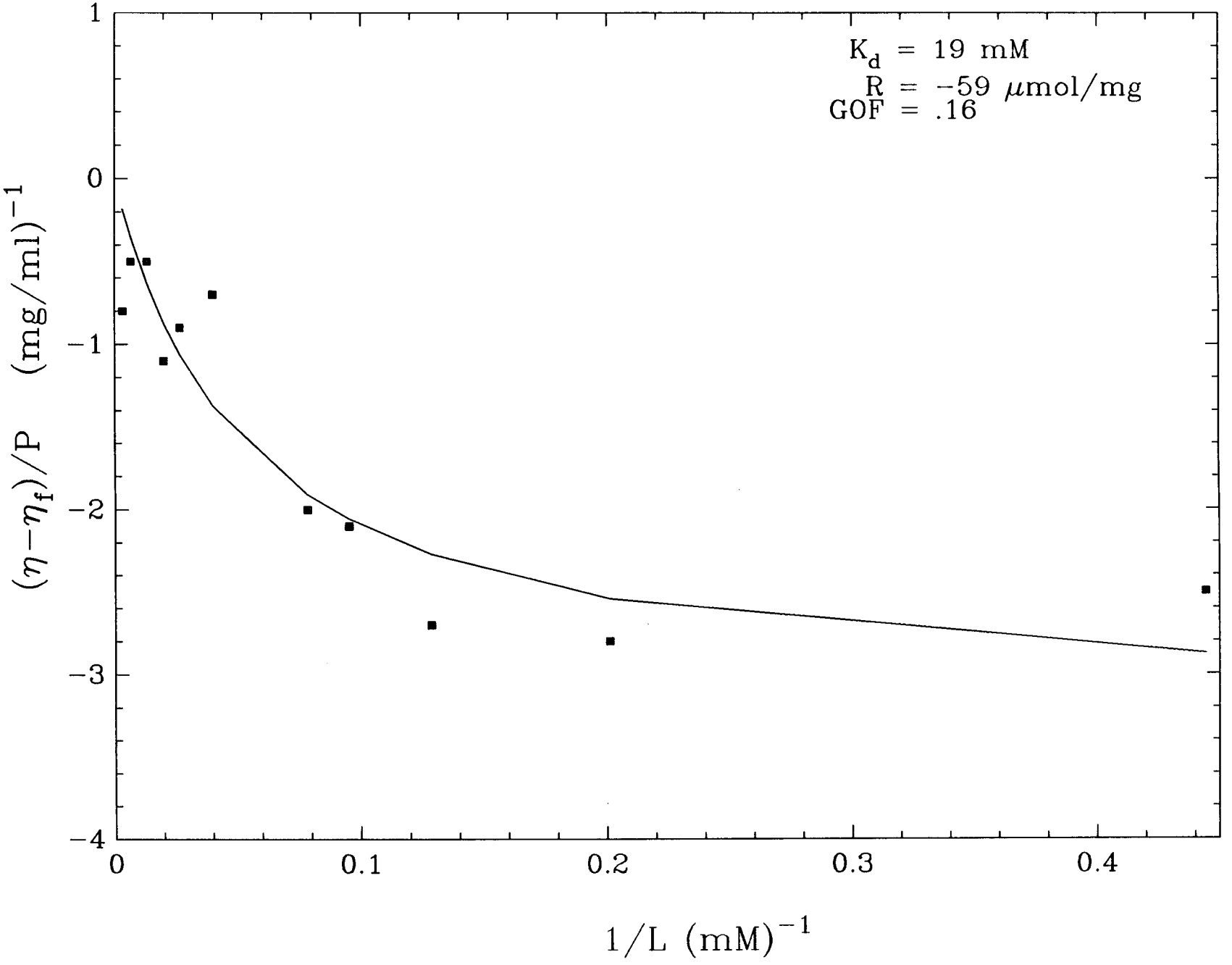
K_d = 19 mM
R = −59 μmol/mg
GOF = .16
$(\eta-\eta_f)/P$ (mg/ml)$^{-1}$
1
0
−1
−2
−3
−4
0
0.1
0.2
0.3
0.4
1/L (mM)$^{-1}$

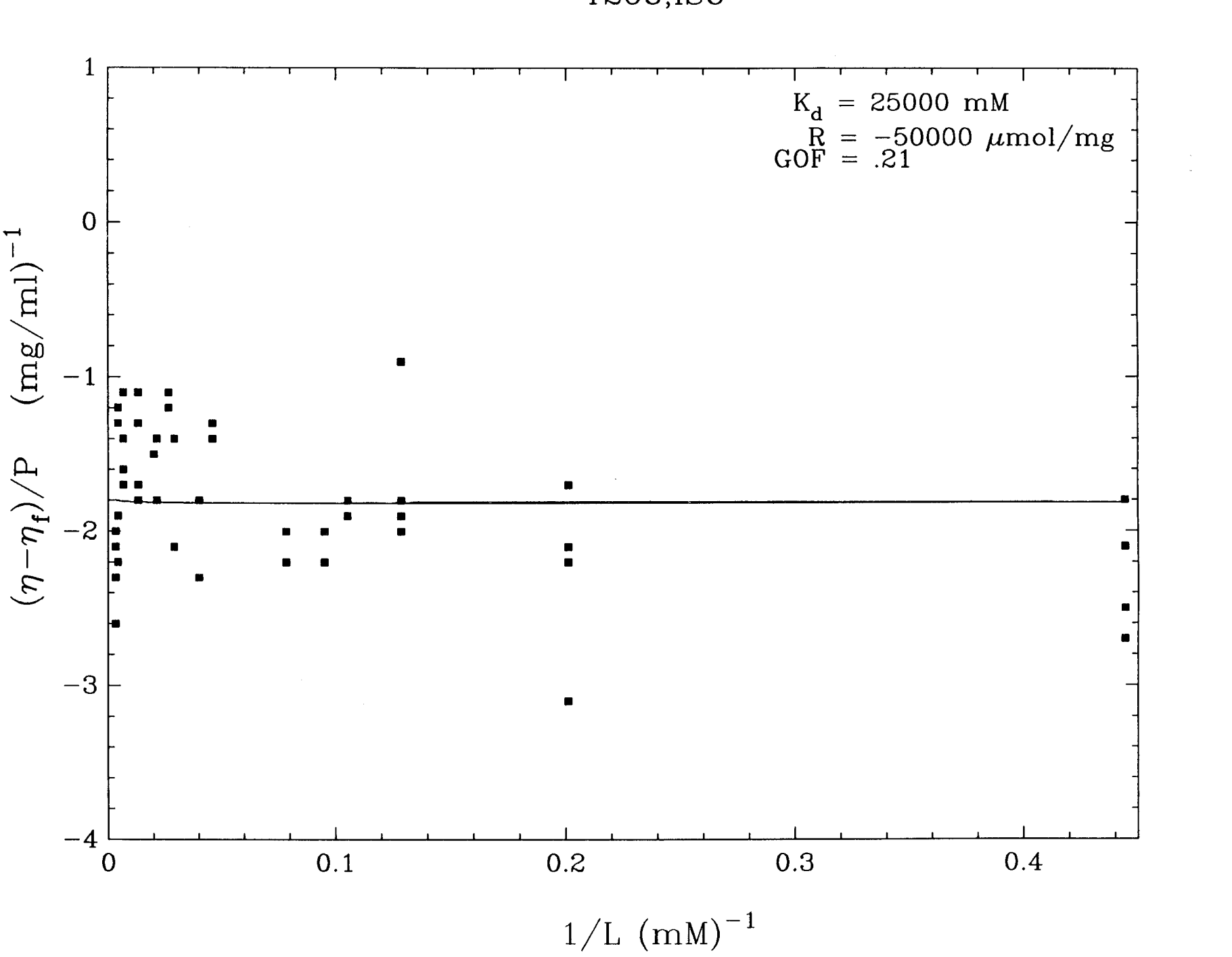
T206,ISO
K_d = 25000 mM
R = −50000 μmol/mg
GOF = .21
$(\eta-\eta_f)/P$ (mg/ml)$^{-1}$
1/L (mM)$^{-1}$
1
0
−1
−2
−3
−4
0
0.1
0.2
0.3
0.4

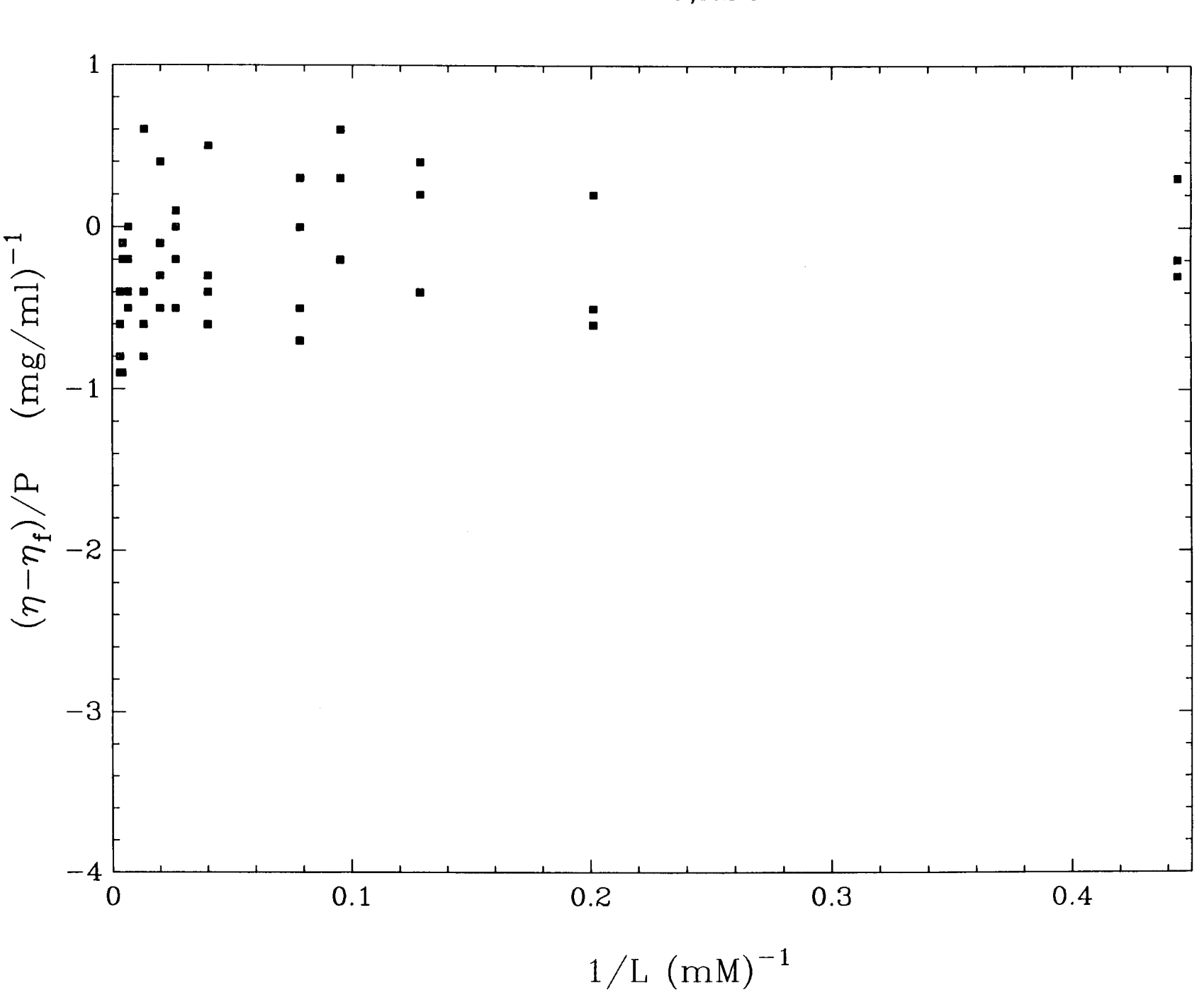
T184,RSO
1
0
−1
−2
−3
−4
0
0.1
0.2
0.3
0.4
$(\eta-\eta_f)/P$ $(mg/ml)^{-1}$
$1/L\ (mM)^{-1}$

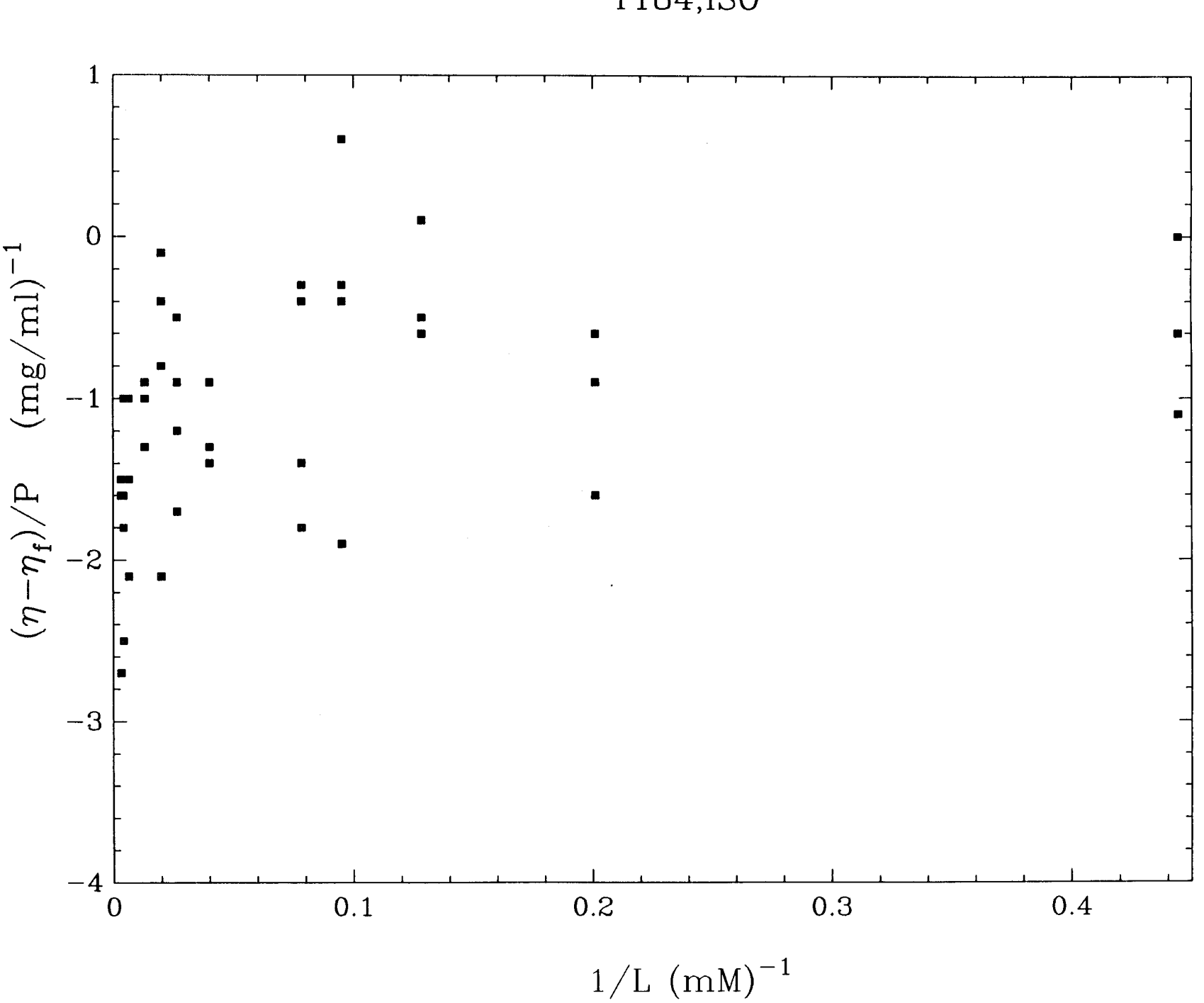
T184,ISO
1
0
−1
−2
−3
−4
0
0.1
0.2
0.3
0.4
$(\eta-\eta_f)/P$ $(mg/ml)^{-1}$
$1/L\ (mM)^{-1}$

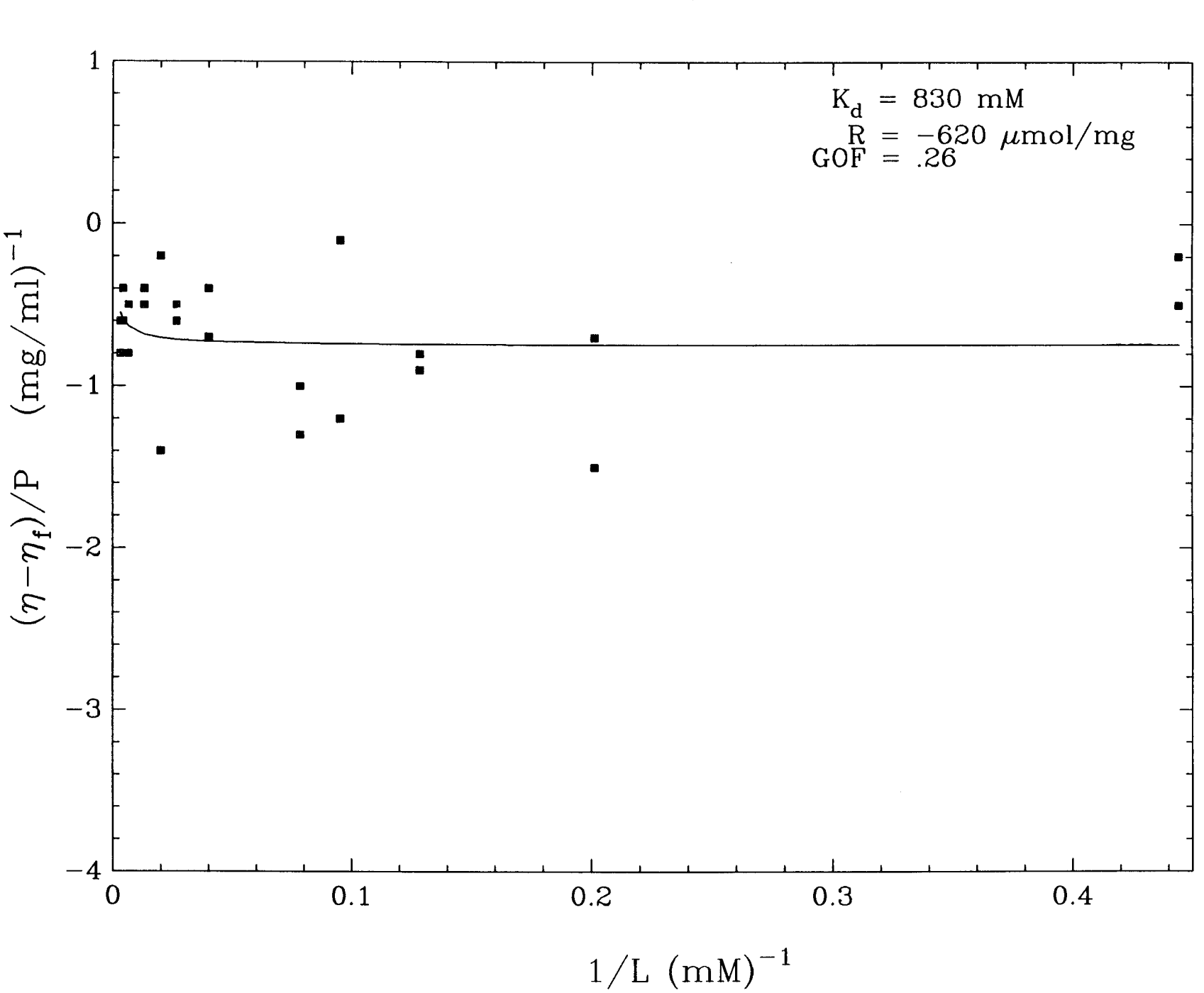
L302,RSO
K_d = 830 mM
R = −620 μmol/mg
GOF = .26
$(\eta-\eta_f)/P$ $(mg/ml)^{-1}$
1
0
−1
−2
−3
−4
0
0.1
0.2
0.3
0.4
$1/L\ (mM)^{-1}$

S148,RSO

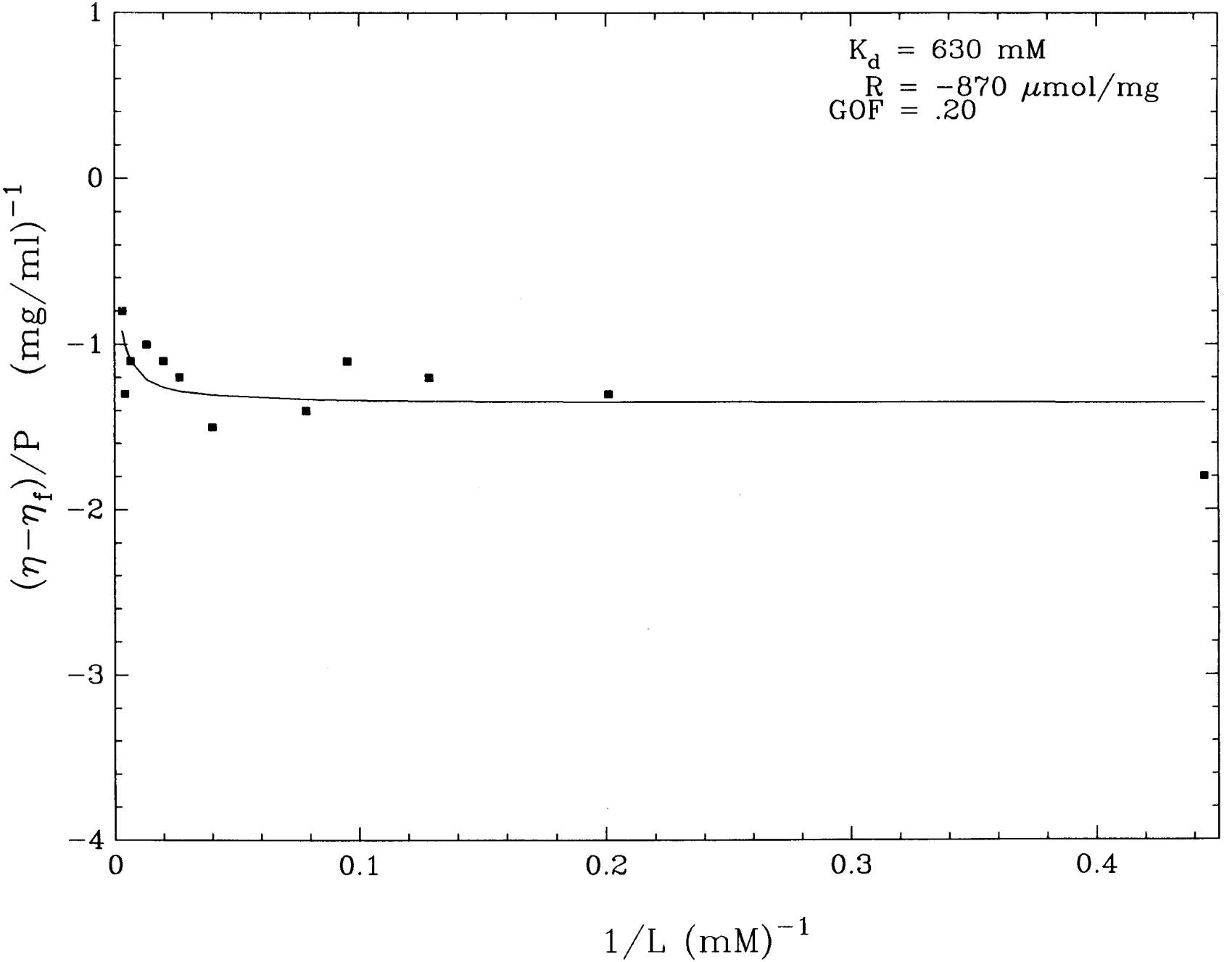
K_d = 630 mM
R = −870 μmol/mg
GOF = .20
1
0
−1
−2
−3
−4
0
0.1
0.2
0.3
0.4
$(\eta-\eta_f)/P$ (mg/ml)$^{-1}$
1/L (mM)$^{-1}$

S148,RSO

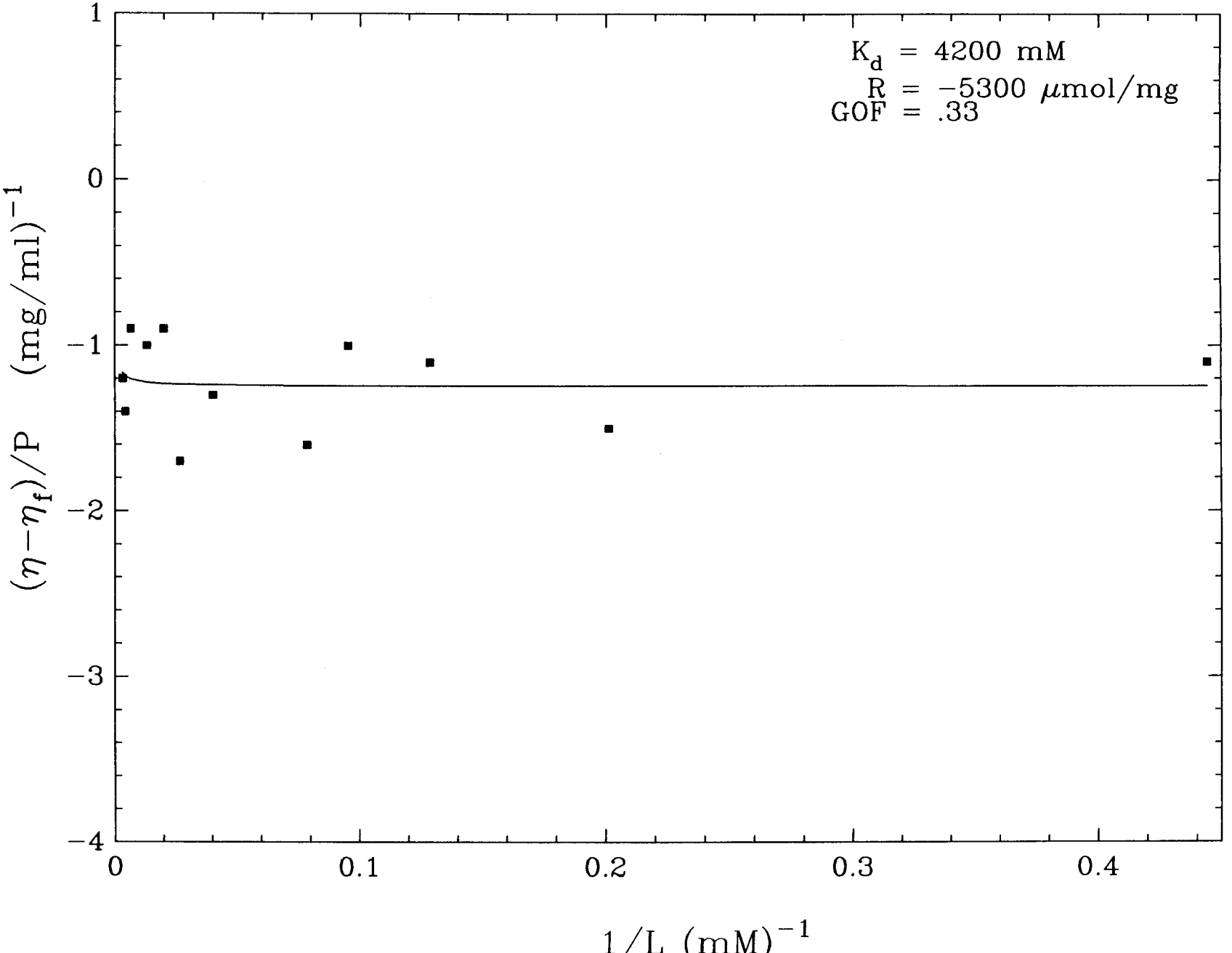
K_d = 4200 mM
R = −5300 μmol/mg
GOF = .33
$(\eta-\eta_f)/P$ (mg/ml)$^{-1}$
1/L (mM)$^{-1}$
1
0
−1
−2
−3
−4
0
0.1
0.2
0.3
0.4

S148,RSO

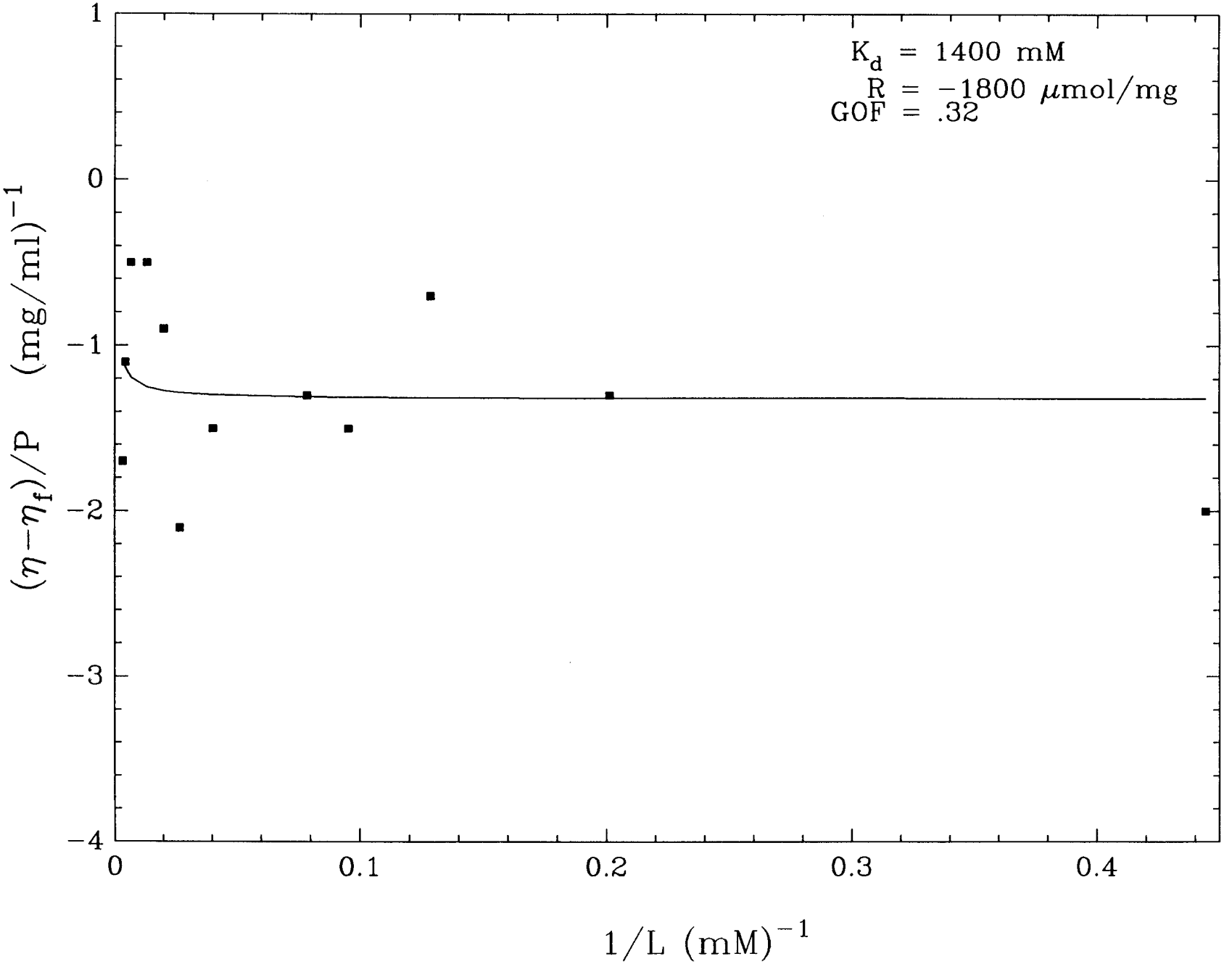
K_d = 1400 mM
R = −1800 μmol/mg
GOF = .32
$(\eta-\eta_f)/P$ (mg/ml)$^{-1}$
1/L (mM)$^{-1}$
1
0
−1
−2
−3
−4
0
0.1
0.2
0.3
0.4

R322,RSO

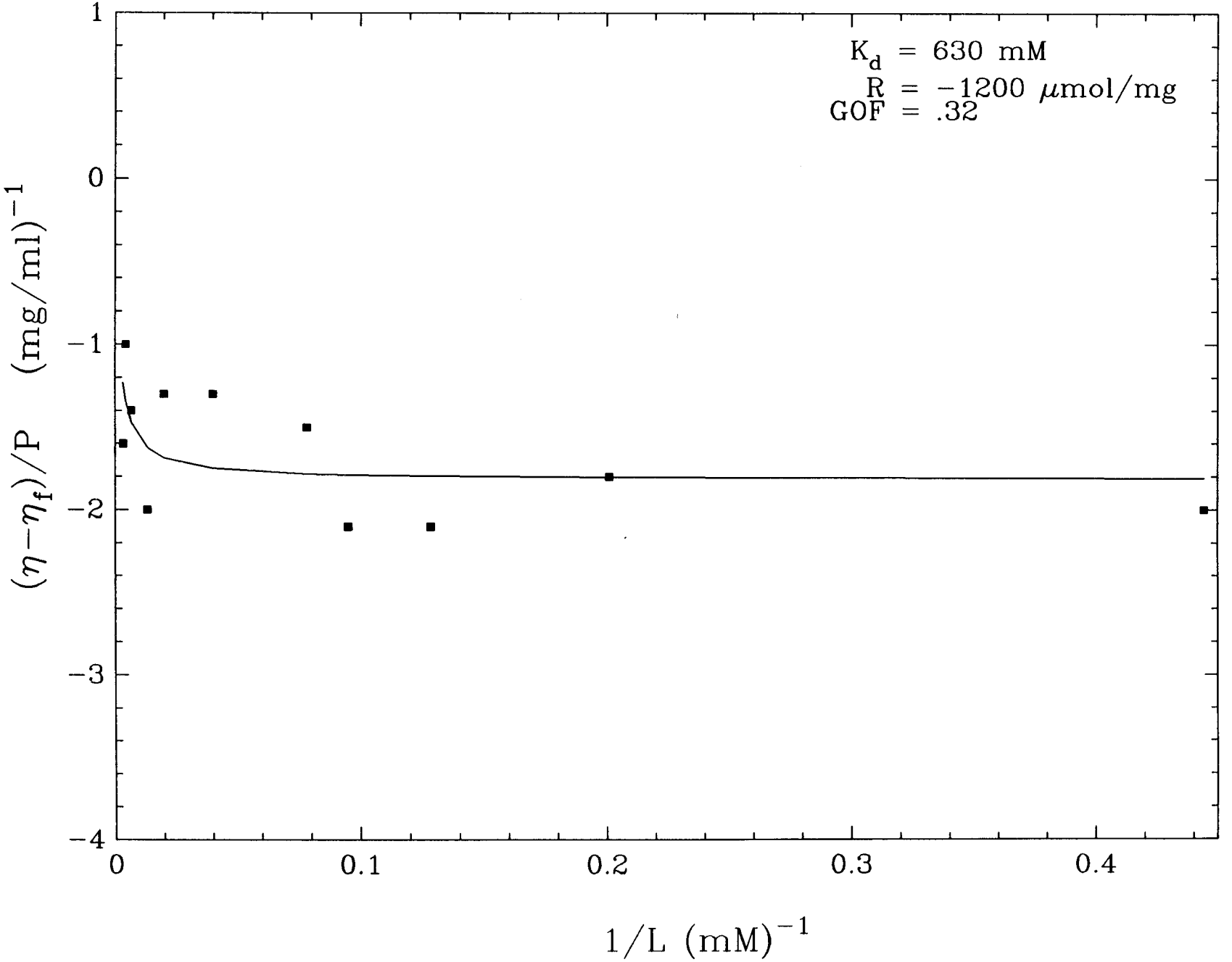
K_d = 630 mM
R = −1200 μmol/mg
GOF = .32
$(\eta-\eta_f)/P$ (mg/ml)$^{-1}$
1/L (mM)$^{-1}$
1
0
−1
−2
−3
−4
0
0.1
0.2
0.3
0.4

R322,RS0

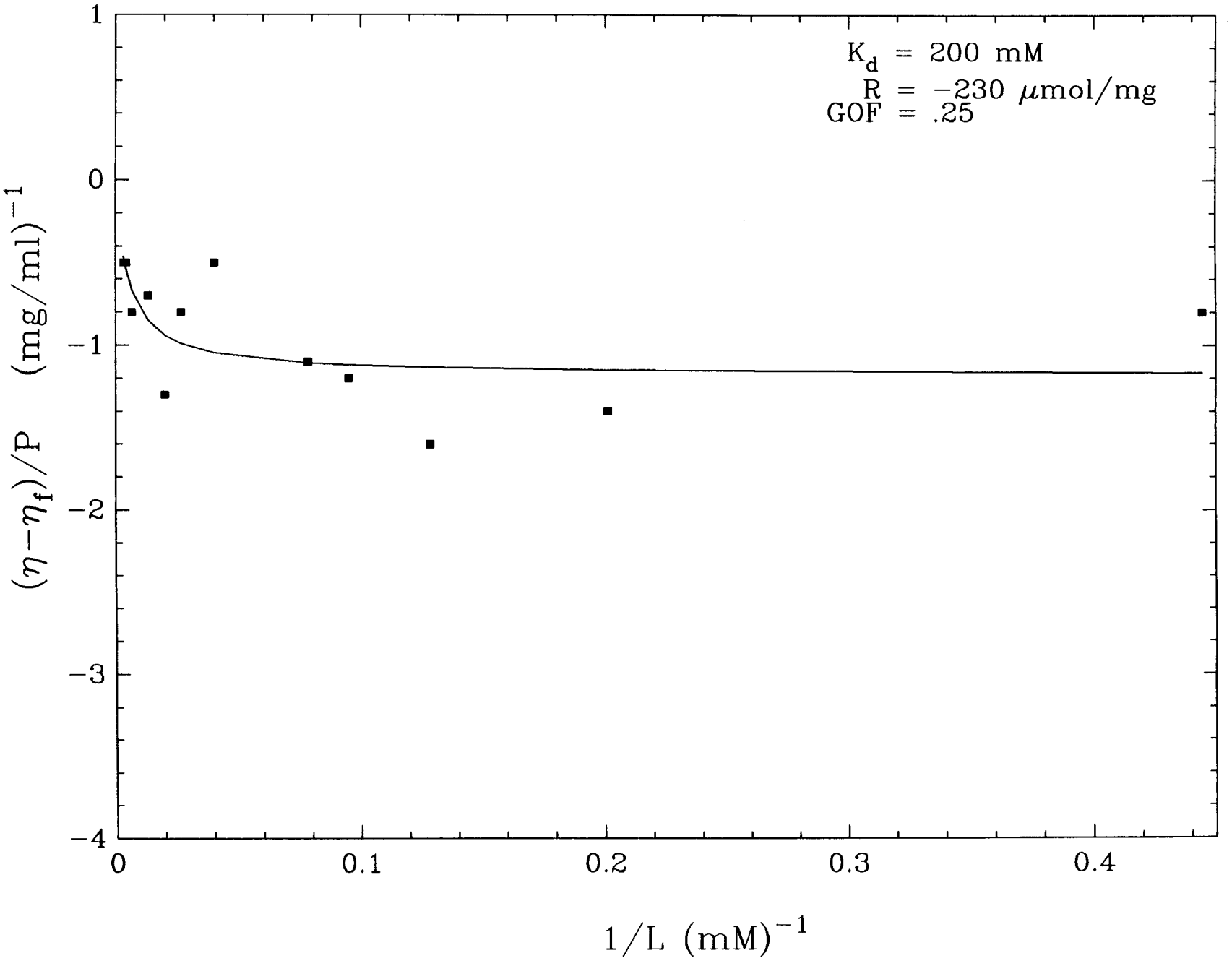
K_d = 200 mM
R = −230 μmol/mg
GOF = .25
$(\eta-\eta_f)/P$ $(mg/ml)^{-1}$
1
0
−1
−2
−3
−4
0
0.1
0.2
0.3
0.4
$1/L\ (mM)^{-1}$

R322,RSO

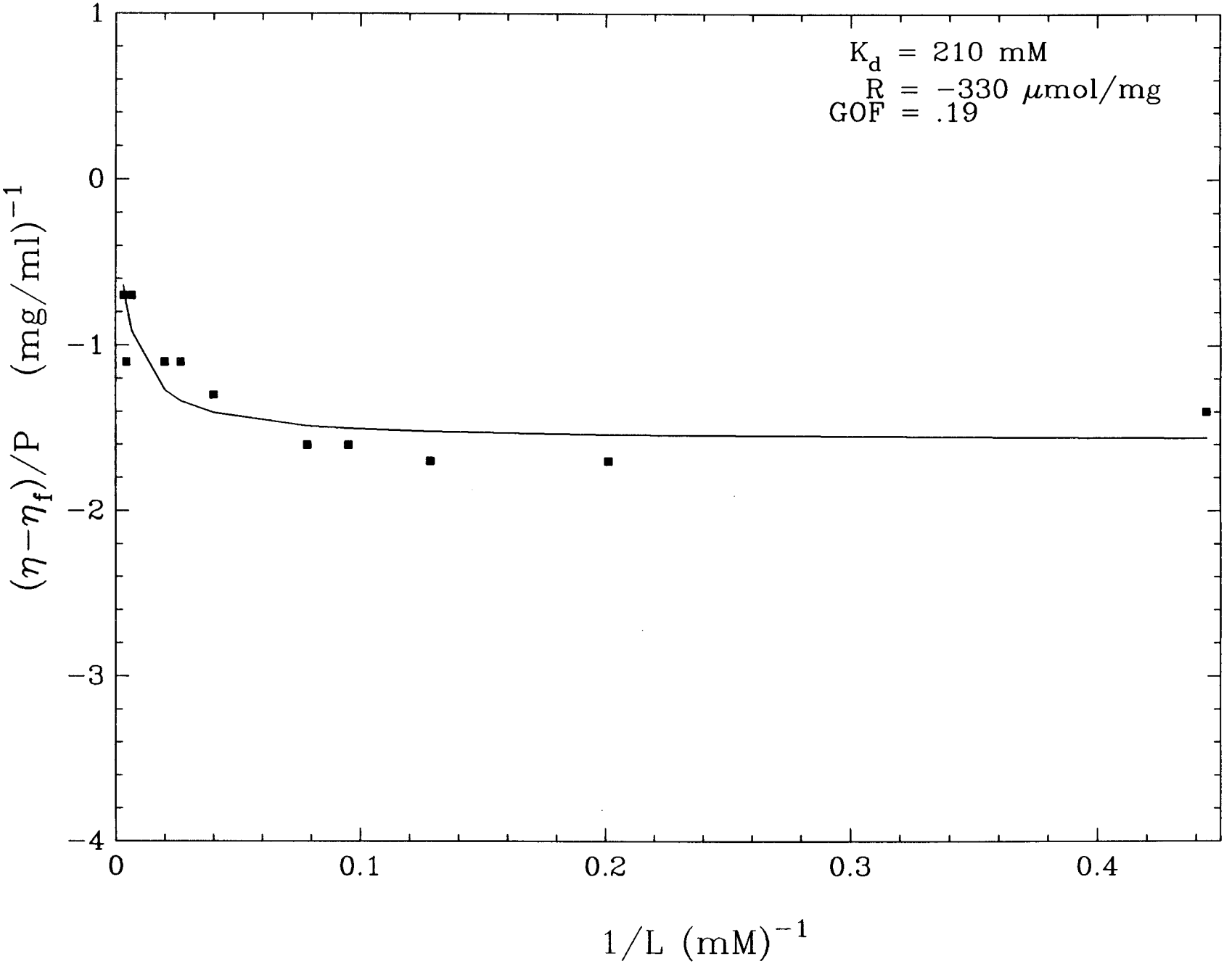
K_d = 210 mM
R = −330 μmol/mg
GOF = .19
$(\eta-\eta_f)/P$ (mg/ml)$^{-1}$
1
0
−1
−2
−3
−4
0
0.1
0.2
0.3
0.4
1/L (mM)$^{-1}$

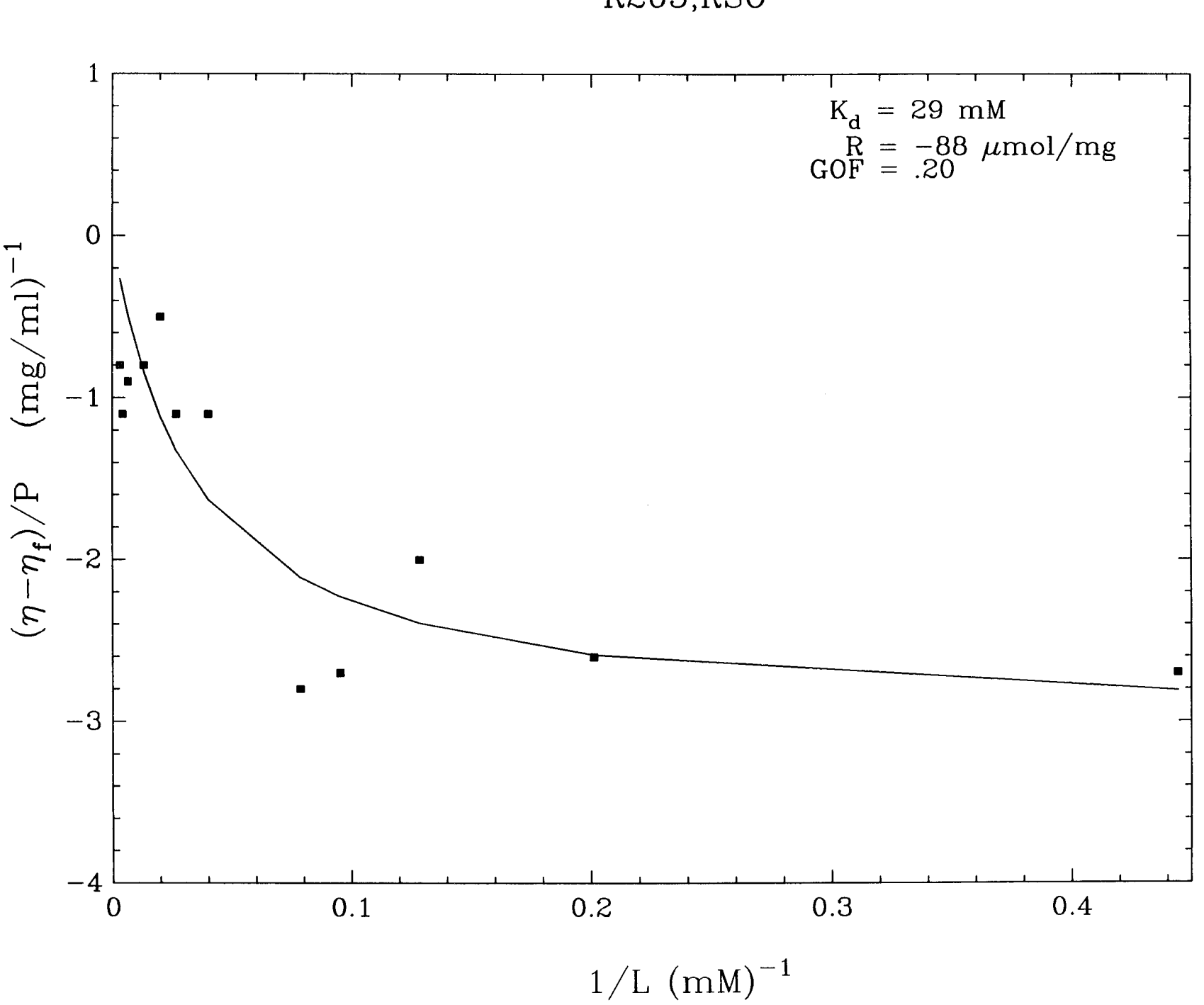
R205,RSO
K_d = 29 mM
R = −88 μmol/mg
GOF = .20
$(\eta-\eta_f)/P$ (mg/ml)$^{-1}$
1/L (mM)$^{-1}$
1
0
−1
−2
−3
−4
0
0.1
0.2
0.3
0.4

R205,RSO

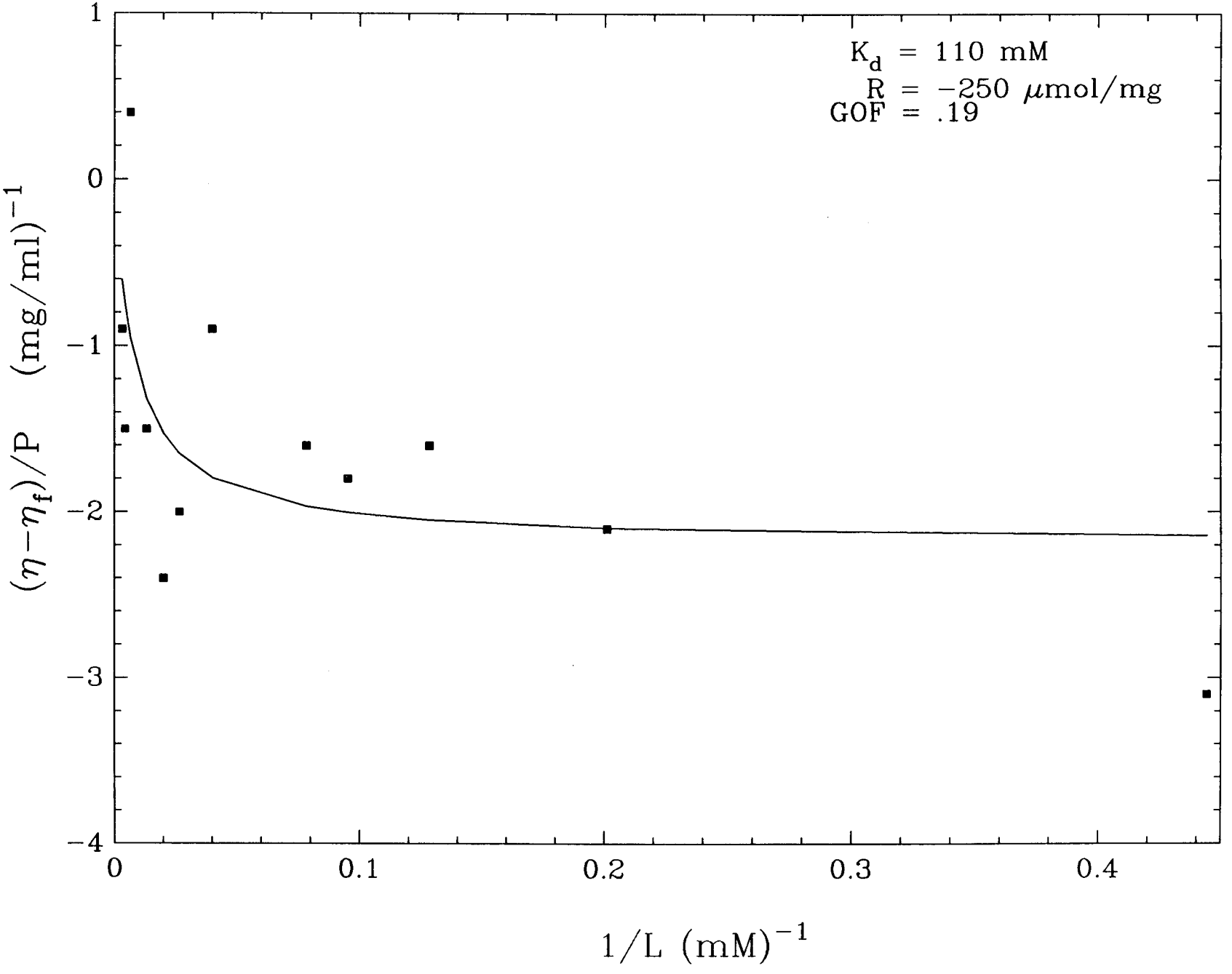
K_d = 110 mM
R = −250 μmol/mg
GOF = .19
$(\eta-\eta_f)/P$ (mg/ml)$^{-1}$
1
0
−1
−2
−3
−4
0
0.1
0.2
0.3
0.4
1/L (mM)$^{-1}$

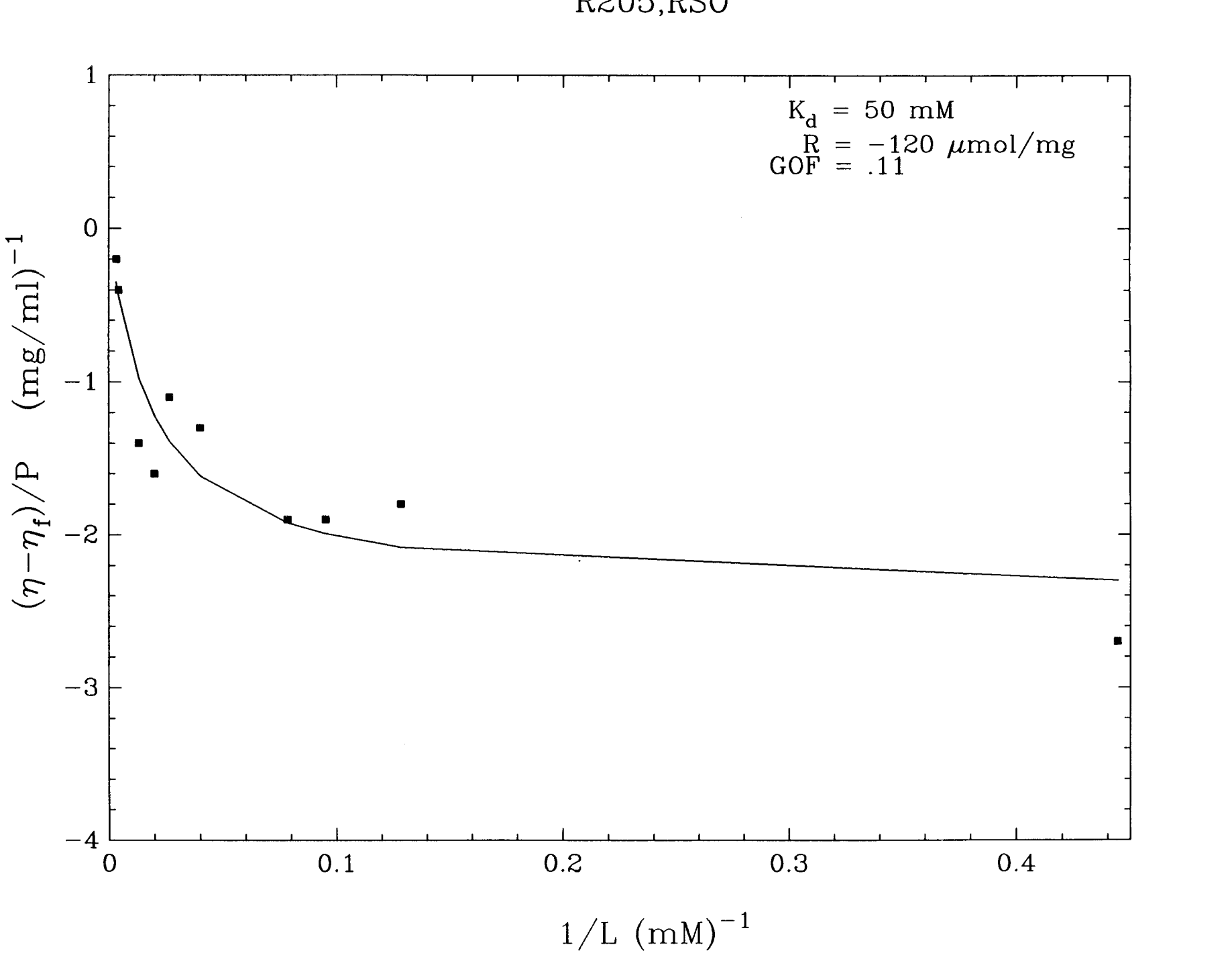
R205,RSO
K_d = 50 mM
R = −120 μmol/mg
GOF = .11
$(\eta-\eta_f)/P$ (mg/ml)$^{-1}$
1/L (mM)$^{-1}$
1
0
−1
−2
−3
−4
0
0.1
0.2
0.3
0.4

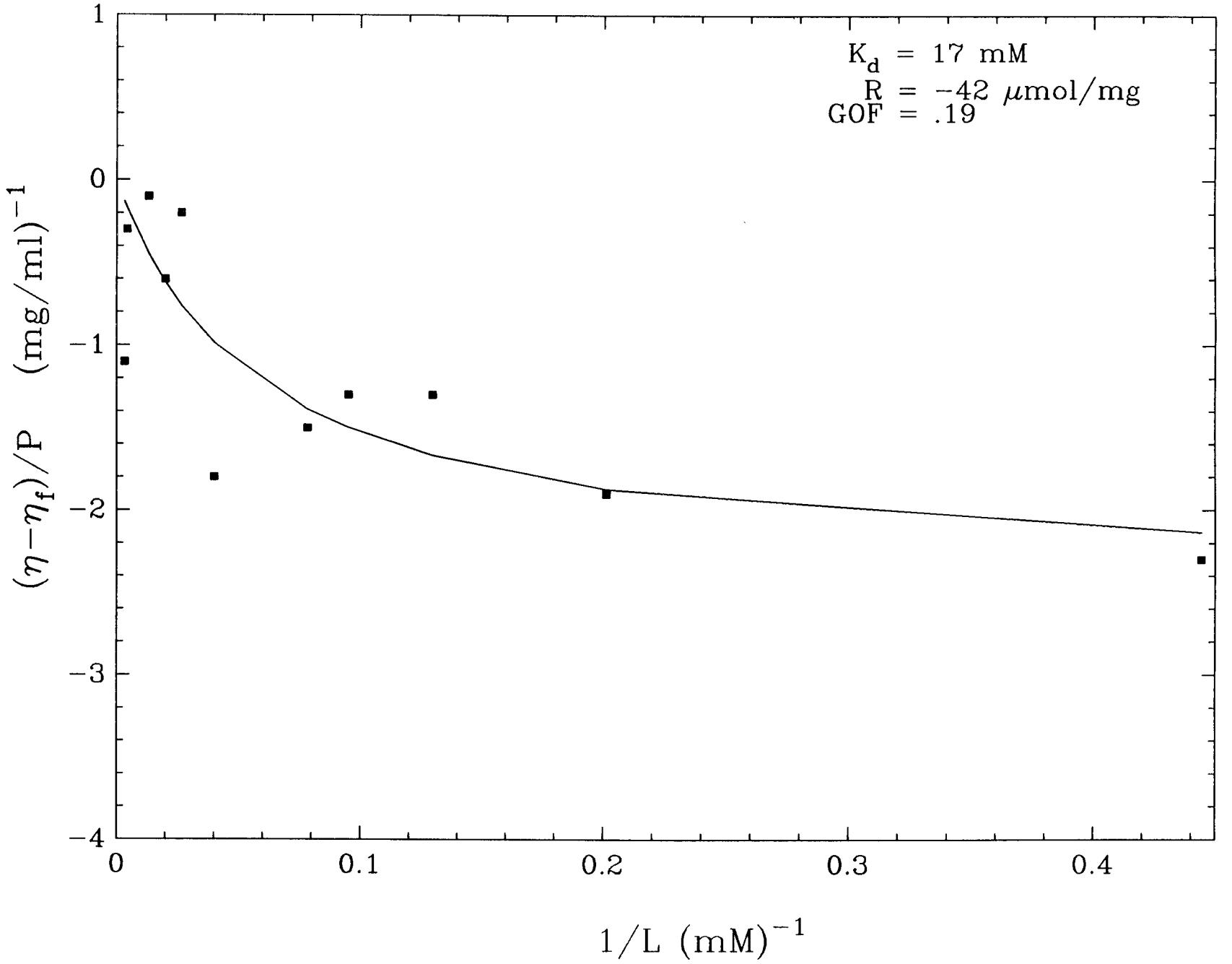
RQHE,RSO
K_d = 17 mM
R = −42 μmol/mg
GOF = .19
$(\eta-\eta_f)/P$ (mg/ml)$^{-1}$
1
0
−1
−2
−3
−4
0
0.1
0.2
0.3
0.4
1/L (mM)$^{-1}$

RQHE,RSO

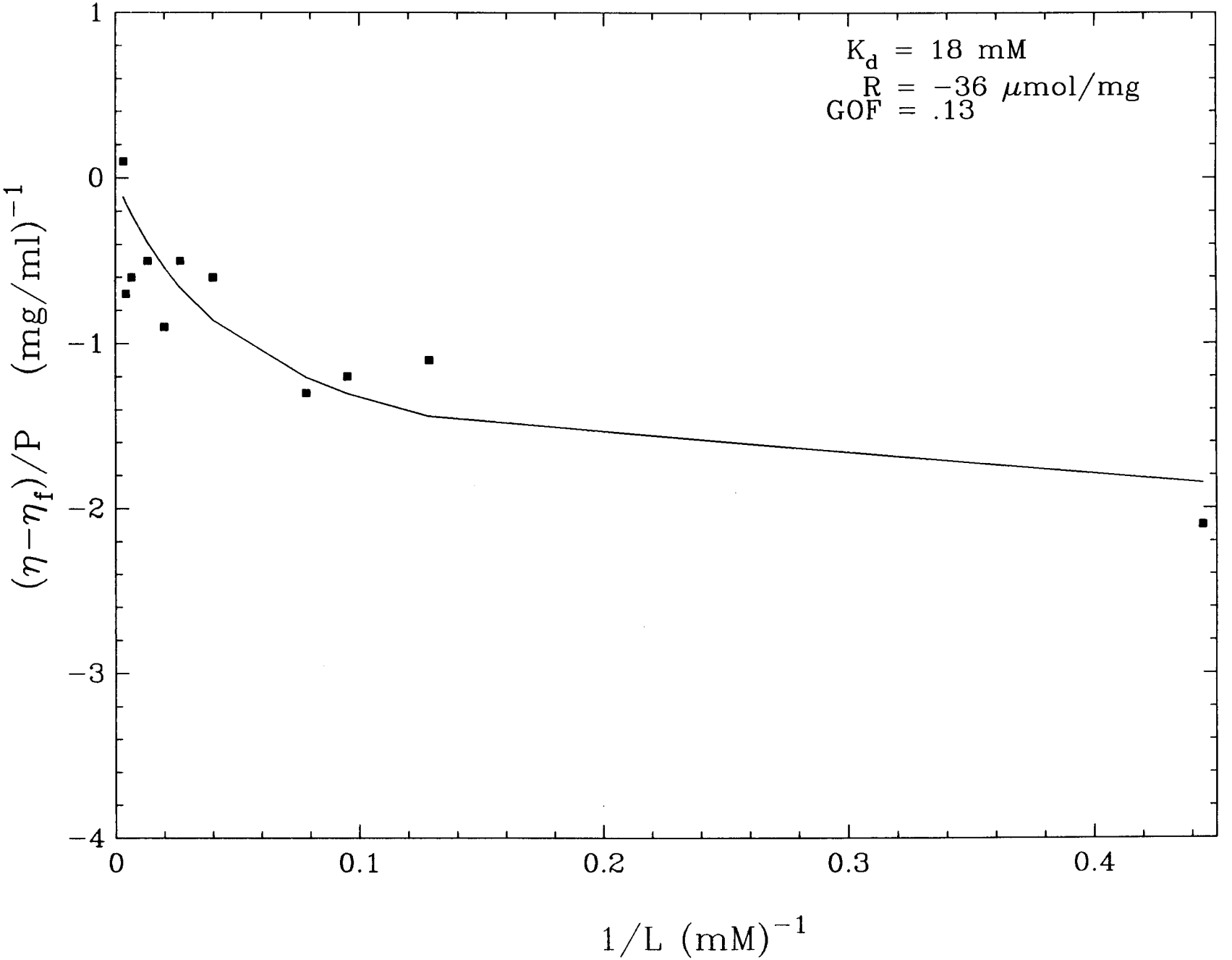
K_d = 18 mM
R = −36 μmol/mg
GOF = .13
1
0
−1
−2
−3
−4
0
0.1
0.2
0.3
0.4
$(\eta-\eta_f)/P$ (mg/ml)$^{-1}$
1/L (mM)$^{-1}$

RQHE,RSO

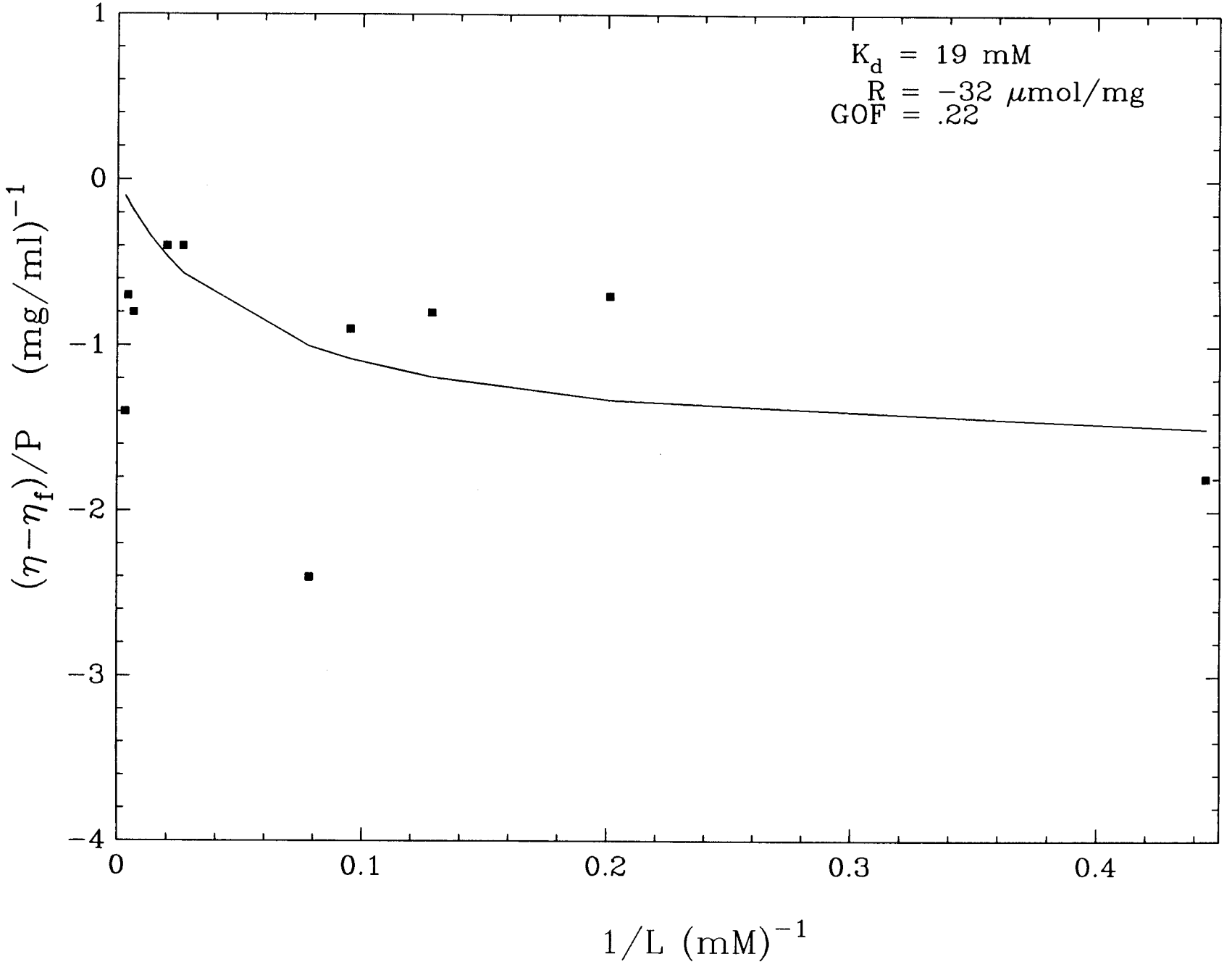
K_d = 19 mM
R = −32 μmol/mg
GOF = .22
$(\eta-\eta_f)/P$ (mg/ml)$^{-1}$
1/L (mM)$^{-1}$
1
0
−1
−2
−3
−4
0
0.1
0.2
0.3
0.4

RQHE,RSO

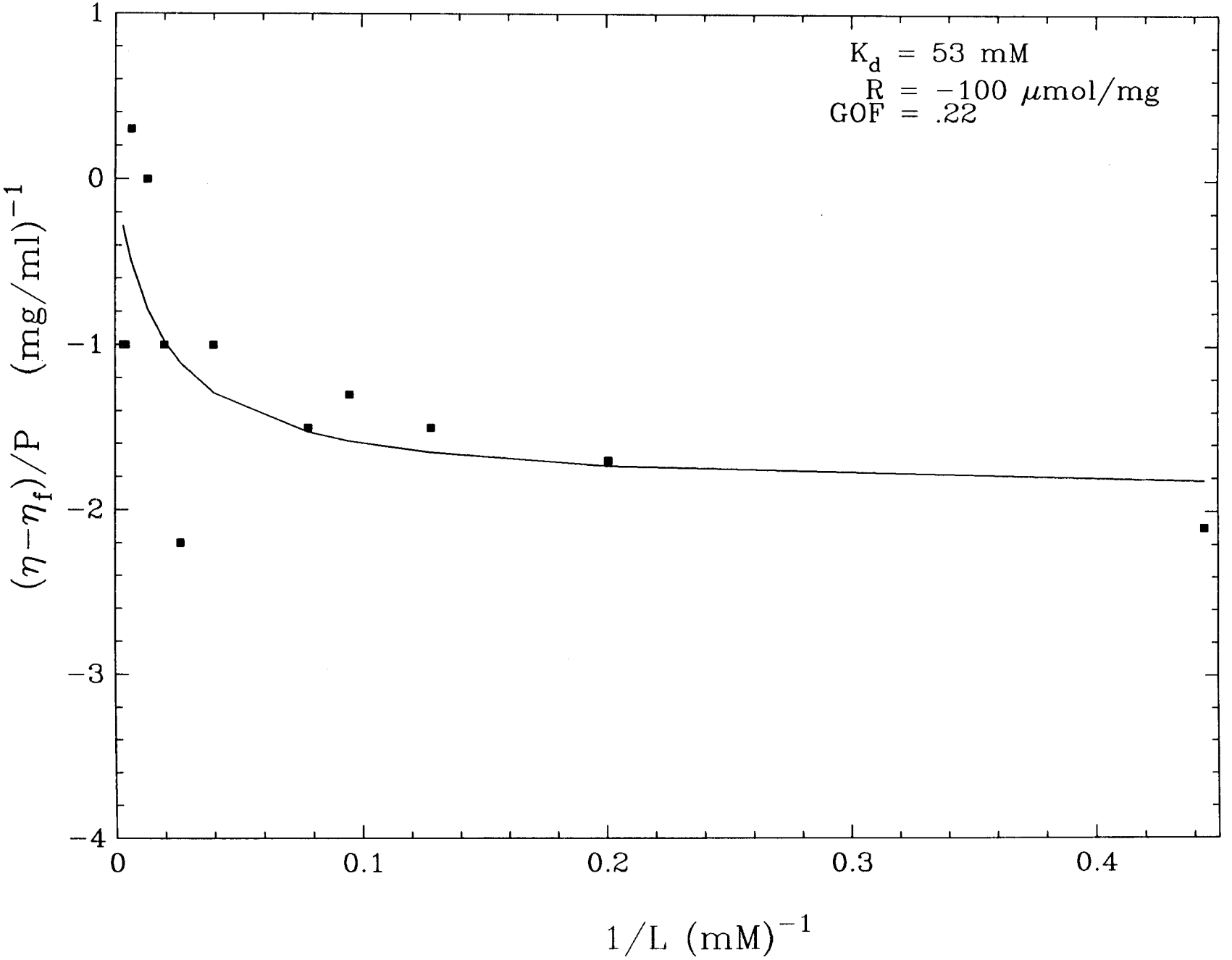
K_d = 53 mM
R = −100 μmol/mg
GOF = .22
$(\eta-\eta_f)/P$ (mg/ml)$^{-1}$
1/L (mM)$^{-1}$
1
0
−1
−2
−3
−4
0
0.1
0.2
0.3
0.4

RQHA,RSO

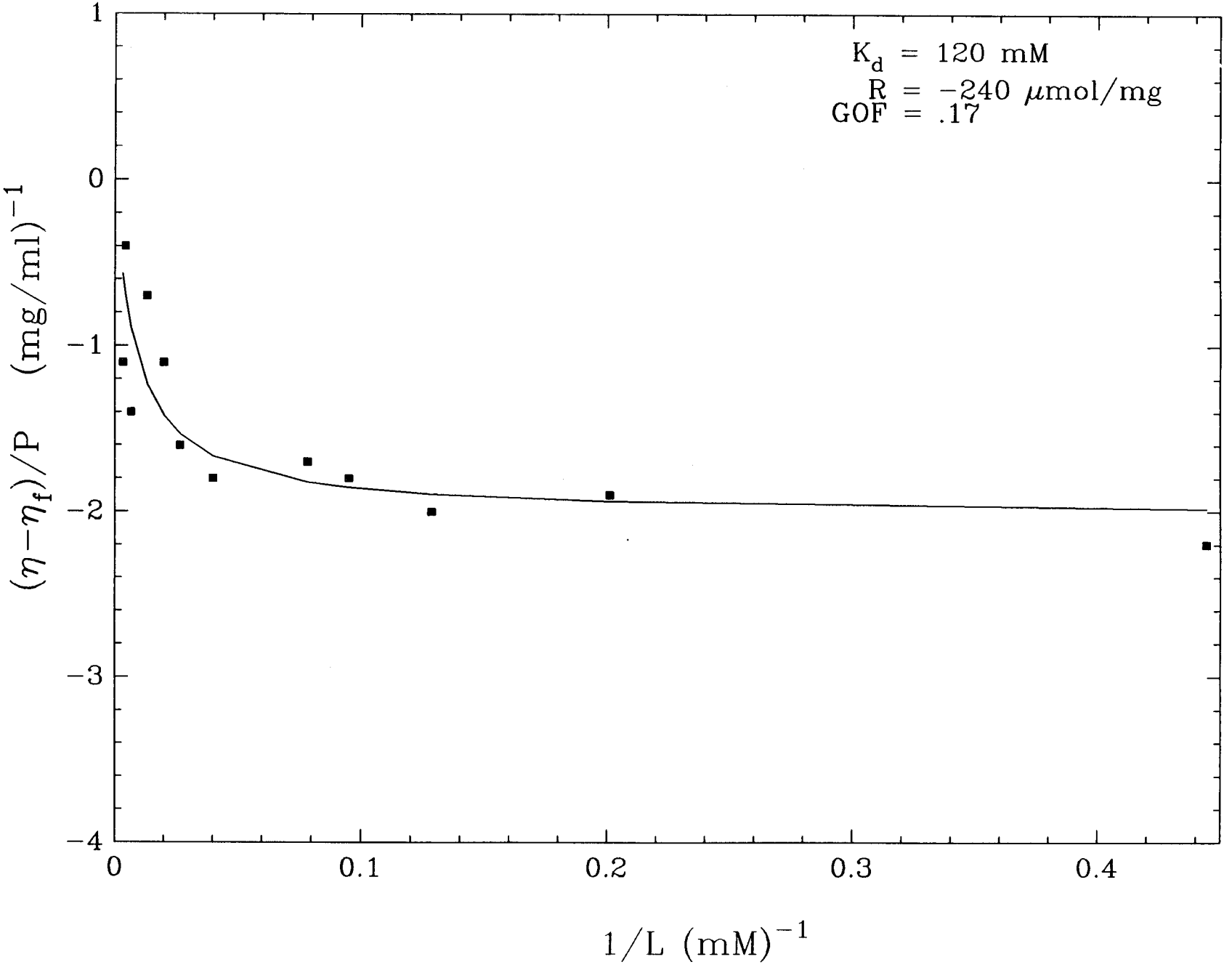
K_d = 120 mM
R = −240 μmol/mg
GOF = .17
$(\eta-\eta_f)/P$ (mg/ml)$^{-1}$
1/L (mM)$^{-1}$
1
0
−1
−2
−3
−4
0
0.1
0.2
0.3
0.4

RQHA,RSO

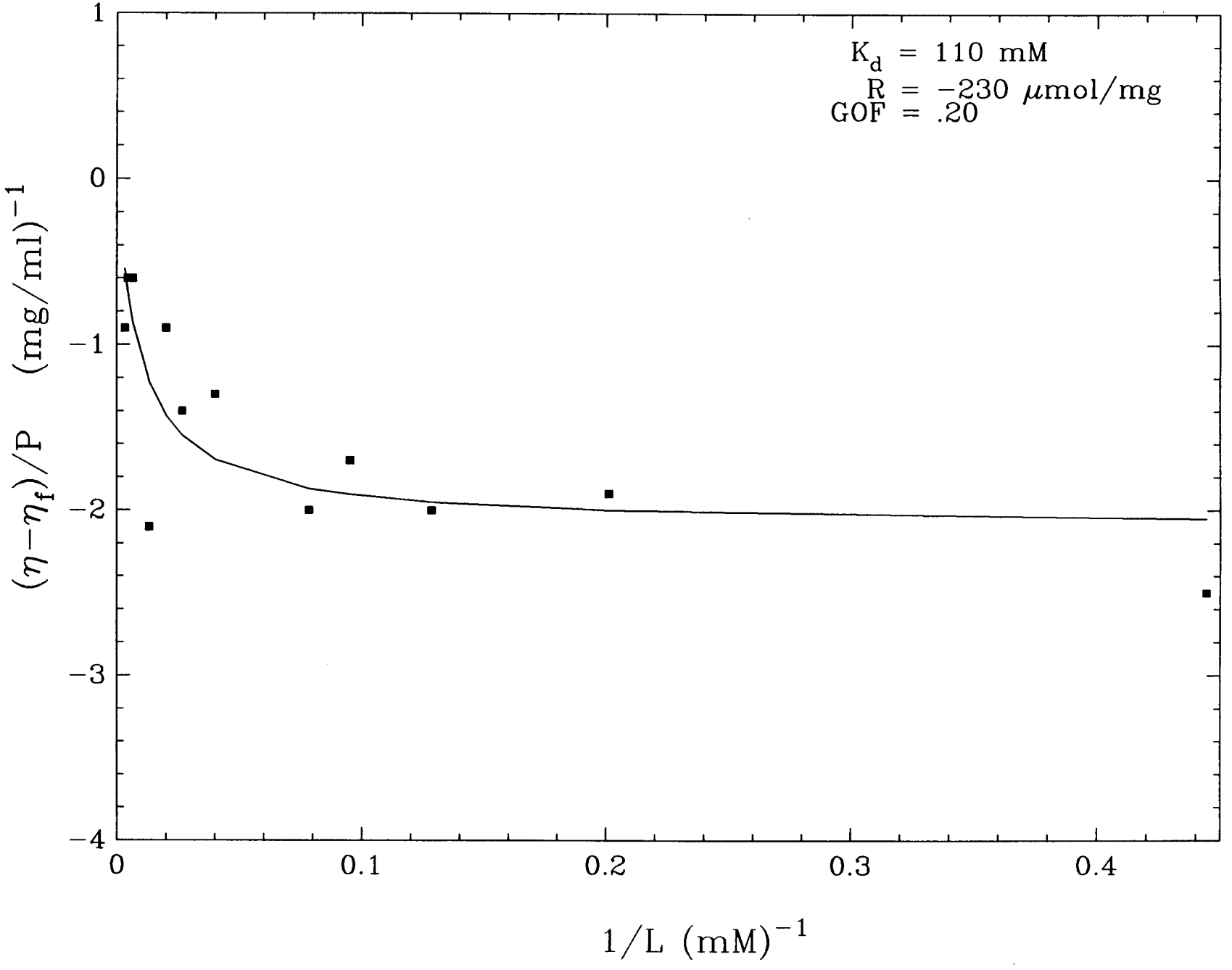
K_d = 110 mM
R = −230 μmol/mg
GOF = .20
1
0
−1
−2
−3
−4
0
0.1
0.2
0.3
0.4
$(\eta-\eta_f)/P$ (mg/ml)$^{-1}$
1/L (mM)$^{-1}$

RQHA,RSO

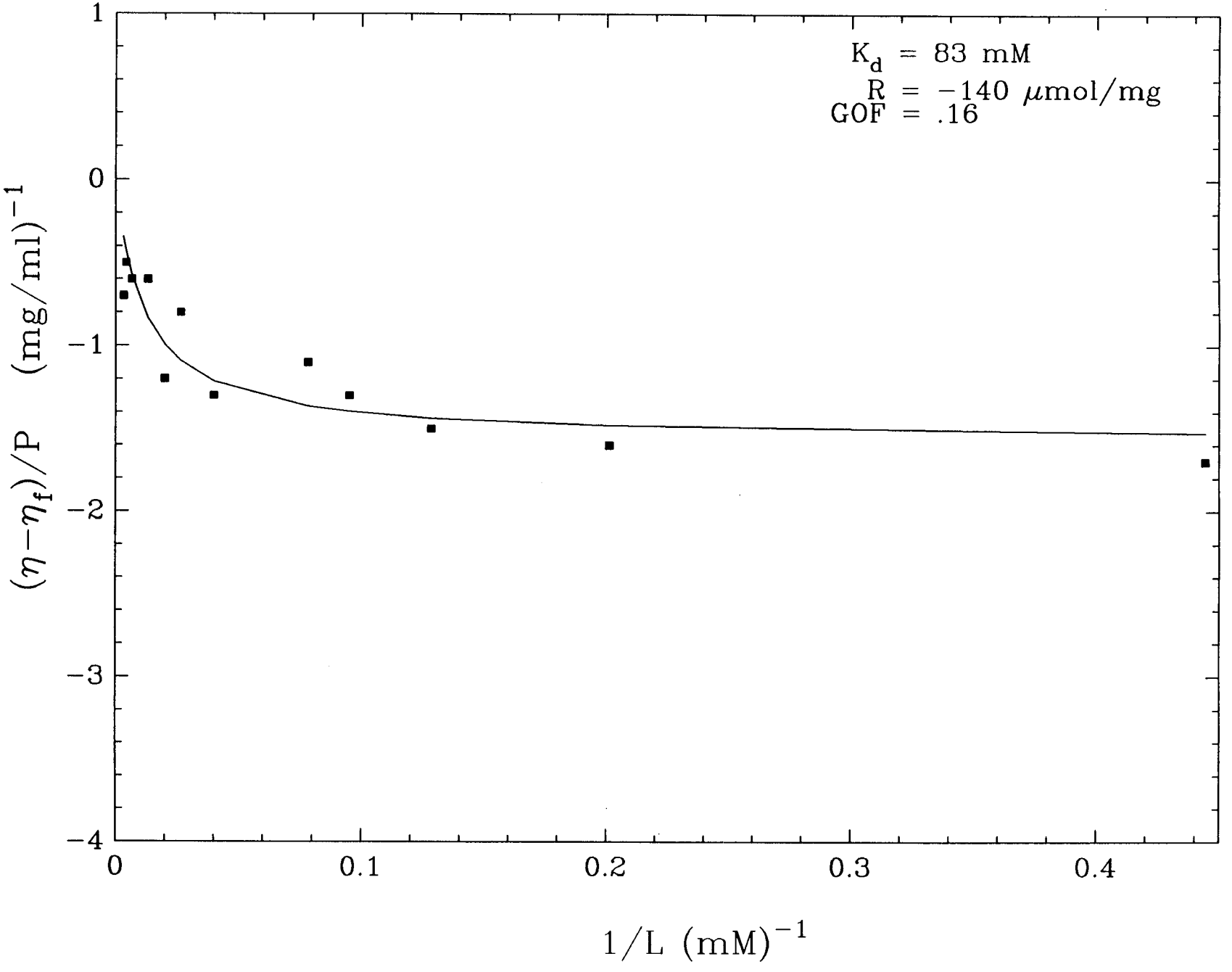
K_d = 83 mM
R = −140 μmol/mg
GOF = .16
1
0
−1
−2
−3
−4
0
0.1
0.2
0.3
0.4
$(\eta-\eta_f)/P$ $(mg/ml)^{-1}$
$1/L\ (mM)^{-1}$

RQHA,RSO

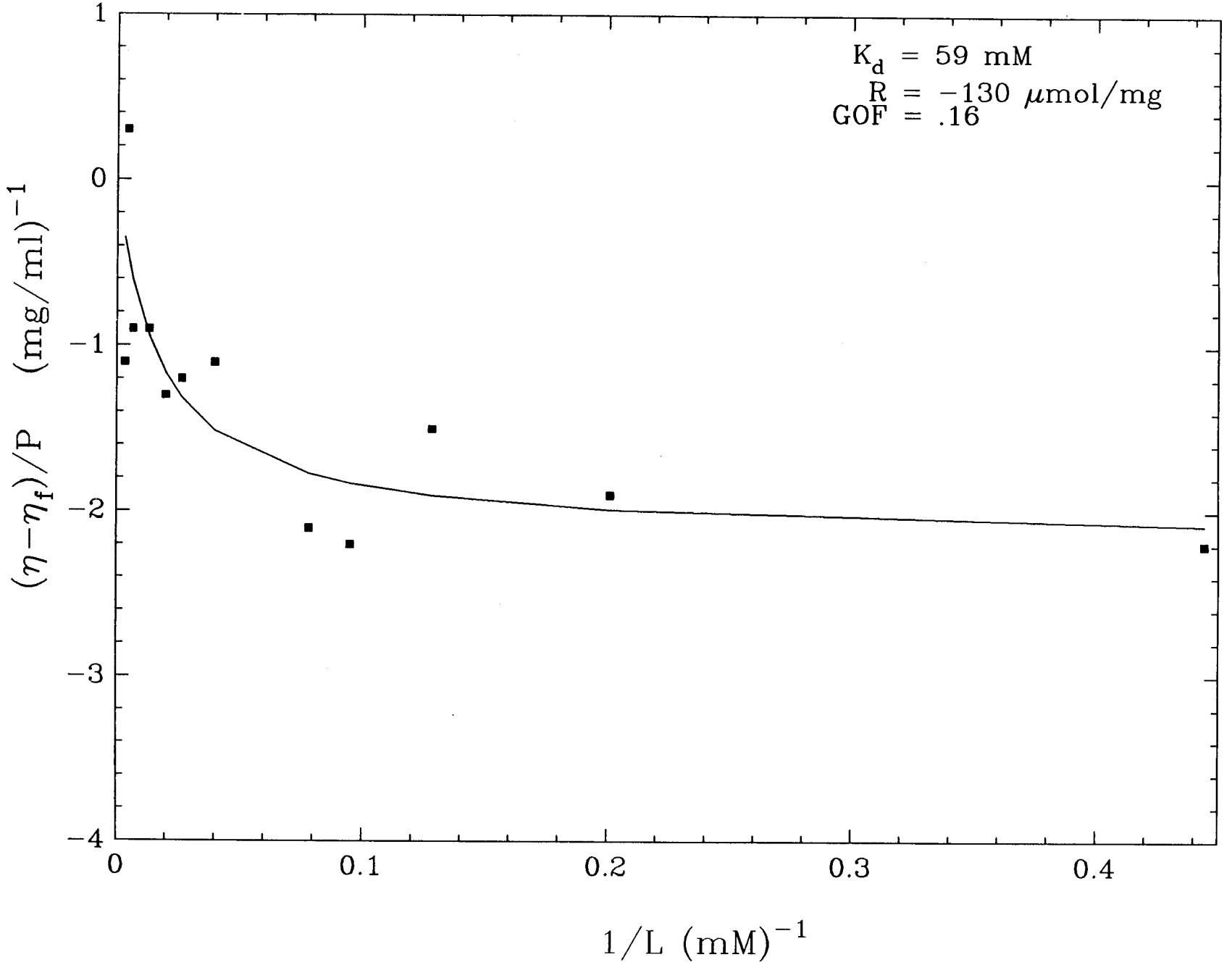
K_d = 59 mM
R = −130 μmol/mg
GOF = .16
$(\eta-\eta_f)/P$ (mg/ml)$^{-1}$
1/L (mM)$^{-1}$
1
0
−1
−2
−3
−4
0
0.1
0.2
0.3
0.4